arXiv:1508.05060v3 [hep-ph] 27 Oct 2015

Consistent constraints on the Standard Model Effective Field Theory

Laure Berthier and Michael Trott
Niels Bohr International Academy, University of Copenhagen, Blegdamsvej 17, DK-2100 Copenhagen, Denmark

ABSTRACT: We develop the global constraint picture in the (linear) effective field theory generalisation of the Standard Model, incorporating data from detectors that operated at PEP, PETRA, TRISTAN, SpS, Tevatron, SLAC, LEPI and LEP II, as well as low energy precision data. We fit one hundred and three observables. We develop a theory error metric for this effective field theory, which is required when constraints on parameters at leading order in the power counting are to be pushed to the percent level, or beyond, unless the cut off scale is assumed to be large, $\Lambda \gtrsim 3\,\mathrm{TeV}$. We more consistently incorporate theoretical errors in this work, avoiding this assumption, and as a direct consequence bounds on some leading parameters are relaxed. We show how an S, T analysis is modified by the theory errors we include as an illustrative example.

Contents

1   Introduction

The linear Standard Model Effective Field Theory (SMEFT) assumes that $SU(2)_L \times U(1)_Y$ is spontaneously broken to $U(1)_{em}$ by the vacuum expectation value of the Higgs field (v) and that the observed 0^+ scalar is embedded in the Higgs doublet. It also assumes that the low energy limit of beyond Standard Model physics (BSM) is adequately described when $SU(3) \times SU(2)_L \times U(1)_Y$ invariant higher dimensional operators built out of the Standard Model (SM) fields, are added to the renormalizable SM interactions.[1] The Lagrangian is schematically

$$\mathcal{L}_{SMEFT} = \mathcal{L}_{SM} + \mathcal{L}_5 + \mathcal{L}_6 + \mathcal{L}_7 + \cdots \tag{1.1}$$

There is one operator in $\mathcal{L}_5$, suppressed by one power of the cut off scale(Λ) [2]. In $\mathcal{L}_6$ there are 59 (+ Hermitian conjugate) operators that preserve Baryon number [3, 4], and four operators that violate Baryon number [2, 5]. $\mathcal{L}_7$ contains twenty operators that all violate lepton number [6]. Recently $\mathcal{L}_8$ has been classified [7] and counts 535 (+ Hermitian conjugate) $N_f = 1$ operators.

The discovery of a 0^+ state at LHC consistent in its properties with the SM Higgs boson, and the lack of discovery of other states proximate in mass to the SM states, implies that the linear SMEFT is a useful and efficient formalism to study and constrain possible deviations from the SM. Determining the global constraints on $\mathcal{L}_6$ is important to inform efforts to search for physics beyond the SM, and will also be a critical consistency check in the event that a beyond the SM state is discovered.[2]

A serious challenge to developing the constraint picture in the general SMEFT is the presence of many unknown parameters. Further, an approach that is inconsistent when considering bounds, for cut off scales in the $\lesssim 3\,\text{TeV}$ range has generally been pursued, as we will show. A key point in the inconsistency is that neglected theoretical errors of the SMEFT can be already dominant in some precisely measured observables, when performing global fits [26]. Unfortunately, if $\Lambda \gtrsim 3\,\text{TeV}$, then it is also unlikely that the impact of corrections to SM predictions, expressed in terms of higher dimensional operators, will be experimentally observable in the near future.[3] As such, to develop applicable and useful constraints it is important to not neglect the theoretical errors we discuss.

---

[1]This later assumption may seem redundant, but is in fact essential. The correct effective field theory, by definition, reproduces the low energy behavior of the underlying theory. It is not guaranteed that the former set of assumptions result in the linear SMEFT framework. The non-linear EFT formalism (including a 0^+ scalar) is a more general approach [1].

[2]The systematic study of the linear SMEFT framework is a subject of growing interest. See Refs. [8–25] for some past global analyses and related discussions.

[3]If a SM symmetry is not violated by the operator.

In this paper we determine constraints on some parameters present in $\mathcal{L}_6$, being careful to ascribe a theoretical error for the various observables. Our approach to Electroweak data is strongly influenced by the pioneering results in Refs. [27, 28]. We incorporate results on scattering data from the detectors that operated at the LEPI, PEP, PETRA, SpS, Tevatron, TRISTAN and LEPII accelerator complexes, as well as low energy data from Atomic Parity Violation and Deep Inelastic Scattering measurements from CHARM, CDHS, CCFR, NuTeV, SLAC E158, eDIS and SAMPLE into a global linear SMEFT analysis.

The outline of this paper is as follows. In Section 2 we lay out our fit methodology, while defining our approach to theory errors. We then present directly in Section 3 our main results concerning LEP data and our global analysis. Most of the details of the analysis are relegated to the Appendix. Our notational conventions are defined in the Appendix and in the companion paper Ref. [26].

A summary of our main conclusions is as follows. The per-mille/few percent constraint hierarchy concerning experimental precision at LEPI and LEPII/LHC does not consistently translate into a hierarchy of constraints on individual leading Wilson coefficients in the SMEFT. Claims on per-mille, or sub-per-mille constraints on all individual $\mathcal{L}_6$ parameters that contribute to LEPI data, are not supported by our results. As a consequence, it is in our view not justified to set these parameters to zero in LHC analyses. This is the case even before SMEFT theoretical errors are included. When these errors are added, the experimental hierarchy in precision is further undermined in its projection into the theoretical parameters. We find that it is important to include SMEFT theory errors when experimental precision reaches the percent level, and critical to include these errors for experimental bounds that report per-mille constraints, when interpreting these bounds model independently in the SMEFT. The differences in fit methodology, observables used, manner of making SM theoretical predictions, and our (more) consistent treatment of theoretical errors explains why our conclusions differ from past results.

2 Constraint methodology

2.1 Operator basis and power counting

We use the well defined operator basis given in Ref. [4] when calculating. We canonically normalize the theory in unitary gauge, taking the theory to the mass eigenstates as in Ref. [29]. For power counting, we use the most general naive power counting, simply suppressing all operators by the appropriate power of the cut off scale Λ. Although alternative schemes of power counting can be self consistent, they are also limited in their applicability.

We adopt the assumption of exact $U(3)^5$ symmetry in the SMEFT corrections. We also adopt the assumption that the Wilson coefficients in $\mathcal{L}_6$, and the loop improved electroweak coupling $\hat{\alpha}$, are real in the analyses we present. These assumptions should also be relaxed, if possible to do so in a consistent manner. For a recent effort aimed at relaxing the $U(3)^5$ assumption, see Ref. [30].

2.2 Fit methodology

Consider a set of observables $\Omega_O = \{O_i\}_{i \in [\![1,n]\!]}$. We denote the measured value of an observable as $\hat{O}_i$ while its predicted value i.e its value in the SMEFT[4] is defined by

$$\bar{O}_i = O_i + \sum_{k=1}^{q} \left[\alpha_{i,k} C_k^6\right] + \mathcal{O}\left(\frac{\bar{v}_T^4}{\Lambda^4}\right), \tag{2.1}$$

where C^6 is a Wilson coefficient of an operator in $\mathcal{L}_6$, while C^8 is a Wilson coefficient of an operator in $\mathcal{L}_8$ etc. Note that the C^6 contain an implicit factor $1/\Lambda^2$. We will sometimes pull this factor out and will write it explicitly as $C^6 \bar{v}_T^2/\Lambda^2$. O_i is the prediction of the observable in the SM. Here $\Omega_C = \{C_k\}$ with $k \in [\![1,q]\!]$ is the set of Wilson coefficients contributing to the shifts of all the O_i. Note that $\alpha_{i,k}$ can be 0 since in general just a subset of the C_k contribute to the shift of an observable O_i. This notation is consistent with the conventions in Ref. [26].

The measured values $\hat{O}_i$ can be regarded as a gaussian variable centred about the predicted value $\bar{O}_i$ following the central limit theorem. Introducing the n dimensional vectors $\hat{O} = (\hat{O}_1, ..., \hat{O}_n)$ and $\bar{O} = (\bar{O}_1, ..., \bar{O}_n)$ we can write the likelihood function which is just the joint probability distribution function (p.d.f), of these n gaussian distributions

$$L(C) = \frac{1}{\sqrt{(2\pi)^n |V|}} \exp\left(-\frac{1}{2}\left(\hat{O} - \bar{O}\right)^T V^{-1} \left(\hat{O} - \bar{O}\right)\right), \tag{2.2}$$

where V is the covariance matrix with elements

$$V_{ij} = \Delta_i^{exp} \rho_{ij}^{exp} \Delta_j^{exp} + \Delta_i^{th} \rho_{ij}^{th} \Delta_j^{th}, \tag{2.3}$$

with the $\rho^{exp,th}$ being the correlation matricies for the experimental and theoretical errors respectively.[5] We have denoted $|V|$ the determinant of the covariance matrix. We separate the experimental and theory errors to avoid introducing incorrect correlation effects.

The Δ_i^{th} is defined as

$$\Delta_i^{th} = \sqrt{\Delta_{i,SM}^2 + (\Delta_{i,SMEFT} \times O_i)^2}, \tag{2.4}$$

where Δ_i^{exp}, $\Delta_{i,SM}$, $\Delta_{i,SMEFT}$ corresponds respectively to the experimental, SM theoretical, and SMEFT theory error for the observable $\bar{O}_i$. Assuming the maximum is found at $L(\tilde{O}_i) = L_{\max}$ the random variable λ defined as

$$\lambda = -2\log\left[\frac{L(O)}{L_{\max}}\right] = \chi^2 - \chi_{\min}^2, \tag{2.5}$$

---

[4]Assuming this is the correct EFT generalization of the SM, and experiment eventually uncovers deviations from the SM.

[5]Formally the covariance matrix V depends on the neglected parameters in the expansion, including dependence on C^6 that is higher order in the power counting. In other words, the dependence on the parameters in the observables fit to is always highly non-linear. Our approach is to approximate all of this implicit dependence on the parameters in higher order terms in the EFT expansion with a numerical error assigned to V. We note that alternative procedures where the implicit dependence on the C_6 parameters in Δ_i is made explicit, are (possibly) also consistent.

has a chi square distribution with number of degrees of freedom $\nu = r$, where r is the number of actual fitted parameters. The value of r may differ from the total number of Wilson coefficients, which is $\dim(\Omega_C) = q$. In 2.5, χ^2 is expanded as

$$
\begin{aligned}
\chi^2 = \sum_{i,j=1}^{n} \left(\hat{O}_i - O_i \right)^T (\mathrm{V}^{-1})_{ij} \left(\hat{O}_j - O_j \right) - 2 \sum_{i,j=1}^{n} \left(\hat{O}_i - O_i \right)^T (\mathrm{V}^{-1})_{ij} \left(\sum_{k=1}^{q} \alpha_{j,k} C_k^6 \right) \\
+ \sum_{i,j=1}^{n} \sum_{k,l=1}^{q} \alpha_{i,l} C_l^6 (\mathrm{V}^{-1})_{ij} \alpha_{j,k} C_k^6 + \mathcal{O}\left(\frac{\bar{v}_T^6}{\Lambda^6} \right),
\end{aligned}
\tag{2.6}
$$

using 2.1.

2.3 Experimental errors and SM theory errors

In the following sections we specify our approach to the errors in the global analysis in detail. Our purpose is to make the analysis reproducible and transparent. When we estimate a SM theoretical error directly in this work, we distinguish these estimates with a $\star$ superscript in the data tables.

2.3.1 LEP based data

Generally, the theoretical error for fitting *in the SM* is well known. For LEPI based data, SM theoretical errors were taken to be the ones defined in Ref. [31] for Γ_Z, σ_{had} and R_f and in Ref. [32] for A_{FB}. We have used the values of the input parameters specified in Ref. [26] to generate predictions in the SM for the LEPII based measurements in Tables 3,5,6,8 using ZFITTER. Following Ref. [33] we have assigned an error of 0.53% for $\sigma(e^+e^- \to \mu^+\mu^-)$, 0.61% for $\sigma(e^+e^- \to \tau^+\tau^-)$ and 0.23% for coloured final state pair production when producing the theoretical prediction with ZFITTER for LEPII data. We have assigned an error of $0.01\sqrt{2}$ multiplying the error of the cross section $\sigma_{e^+e^- \to \mu^+\mu^-}$ (resp. $\sigma_{e^+e^- \to \tau^+\tau^-}$) for A_{FB}^μ (resp. A_{FB}^τ) dropping the percentage symbol. This error prescription follows the discussion in Ref. [33]. When the flavour universal BSM case is considered, the weighted least squares average of the $\sigma(e^+e^- \to \mu^+\mu^-)$ and $\sigma(e^+e^- \to \tau^+\tau^-)$ and of A_{FB}^μ and A_{FB}^τ were taken.

We have also checked that the error introduced by propagating the SM errors in the input observables is subdominant to the estimated theoretical error in the SM already included, and specified below for LEPII observables.[6]

2.3.2 TRISTAN, PEP and PETRA

Measurements at energies below the Z pole are of interest when developing the global constraint picture. Different operating energies $(\sqrt{s})$, help resolve the large number of effects that are present when considering $e^+ e^- \to f \bar{f}$ scattering observables.

A challenge to using this data is the legacy theory predictions that the measurements are compared to. For example, consider the results for the TOPAZ collaboration. In Ref. [34]

---

[6]For more discussion on this issue, see Ref. [17].

$R_{qq} = \sigma(e^+ e^- \to q \bar{q})/\sigma(e^+ e^- \to \text{had})$ and A_q^{FB} for $q = b, c$ are reported at the operating energy $\sqrt{s} = 58 \, \text{GeV}$ with a full (experimental) correlation matrix. The SM predictions compared to are leading order predictions, with no theoretical error stated. Reproducing the predictions for R_{qq} and A_q^{FB} with current PDG values of input parameters introduces shifts compared to the quoted theoretical value $\sim 1 \, \sigma$ for the experimental error quoted for R_{qq}. However, the SM predictions are also corrected in a detector and decay mode specific manner [34]. As such, although leading order QCD radiative corrections are modelled with Monte-Carlo tools using JETSET7.3, we consider it reasonable to ascribe a $\sim 1\%$ SM theoretical error, and to use the supplied predictions.

The justification of a $\sim 1\%$ error assignment is that $\alpha_s(\sqrt{s} \simeq 58 \, \text{GeV})/4\pi \sim 1\%$. We assume residual SM theory errors on the modelling of the leading QCD perturbative corrections for quark final state observables at TRISTAN, PEP and PETRA based detectors of this form. For leptonic final states we take a theoretical error estimate of $\sim 1\%$ for cross section measurements and $\sim 0.1\%$ for A^{FB} measurements, in line with the theory errors produced for similar LEPII observables using ZFITTER. In all cases where we estimate a theory error for $\sqrt{s} < \hat{m}_Z$ colliders the error is subdominant to the experimental errors. In the case of TRISTAN, PEP and PETRA the theory error due to the SMEFT generalization of the SM is also expected to be far smaller than the experimental errors. This is however not the case for LEPI measurements.

2.3.3 Correlations

The theoretical correlations are essentially unknown. The experimental correlations between observables are frequently unknown, except in some exceptional circumstances. This limits how precisely leading parameters can be bounded in the SMEFT, although this effect is difficult to quantify. The well measured subset of LEPI data that define the well known LEPI pseudo-observables supply some correlations, which we use. We also use correlations for σ_{had} supplied for LEPII data, and correlations supplied in Ref. [34] for TOPAZ data. We also use correlations for reported low energy couplings $g_{L/R}^2$ given in Ref. [35].

2.4 SMEFT theory error

2.4.1 LEP, TRISTAN, PEP and PETRA

It is also important to include a theoretical error estimate, due to the SMEFT itself [26]. This is in addition to the SM theoretical error. In the SMEFT, when obtaining a bound on an unknown Wilson coefficient in $\mathcal{L}_6$, the following effects are generally neglected:

- Initial and final state radiation effects in the correction to $2 \to 2$ scattering. These corrections still have an approximate universal form [33, 36, 37]

$$\Delta_{IFI,O_i} \simeq \frac{\bar{v}_T^2}{\Lambda^2} \left(4 \, Q_e \, Q_f \frac{\hat{\alpha}_{ew}}{\pi} \log\left(\frac{E_{max}^\gamma}{E_{beam}}\right) \log\left(\frac{1 - \cos\theta}{1 + \cos\theta}\right) \right), \qquad (2.7)$$

for observables O_i. Here E_{max}^γ is the maximum photon energy not removed with isolation cuts on the signal, and $E_{beam} = \sqrt{s}$ is the operating energy. Using the numerical results in Ref. [33] (Table 12) as a guide we estimate

$$\Delta_{IFI,\sigma_{e^+e^- \to \ell\bar{\ell}},A_{FB}^\ell} \simeq 0.02\,\frac{\bar{v}_T^2}{\Lambda^2} \text{ for lepton pair production,} \tag{2.8}$$

$$\Delta_{IFI,\sigma_{e^+e^- \to q\bar{q}},A_{FB}^q} \simeq 0.01\,Q_f\,\frac{\bar{v}_T^2}{\Lambda^2} \text{ for quark pair production.}$$

- Neglected perturbative corrections in the SMEFT. These corrections are currently treated inconsistently in global fits. This requires the introduction of a theoretical error, which we define as

$$\Delta_P \simeq \frac{g_{1,2,3}^2}{16\,\pi^2}\,\left(a + b\log\left(\frac{\mu_1^2}{\mu_2^2}\right)\right)\frac{\bar{v}_T^2}{\Lambda^2}. \tag{2.9}$$

Although the value of b for specific observables can be (mostly) inferred from the Renormalization Group (RG) results for the SMEFT in Ref. [29, 38, 39], the corresponding "a" finite terms are not small enough in general to be neglected at NLO, see Refs. [40–42]. Here $\mu_{1,2}$ are schematic for the characteristic scales. Taking $\mu_1 = \Lambda$, $\mu_2 = v$, $a = b = 1$ and $g = 0.65$ for EW corrections we find an estimate for neglected running effects in the SMEFT

$$\Delta_P \simeq 0.02\frac{\bar{v}_T^2}{\Lambda^2} \text{ for } \Lambda = 3 \text{ TeV}, \qquad \Delta_P \simeq 0.01\frac{\bar{v}_T^2}{\Lambda^2} \text{ for } \Lambda = 1 \text{ TeV}. \tag{2.10}$$

As well as running down from a high scale, there is also the neglect of perturbative corrections in relating input observables to predictions around the electroweak scale. This can correspond to, for example, a scale characterising a low energy measurement of G_F in $\mu^- \to e^- + \bar{\nu}_e + \nu_\mu$ decay ($\sim 10\,\text{GeV}$) compared to a characteristic scale $\sqrt{s} \sim 190\,\text{GeV}$ in a prediction using this measurement. Taking $\mu_2 = 10$ GeV, $\mu_1 = v$, $a = b = 1$ and $g = 0.65$ we get

$$\Delta_{P,II} \simeq 0.02\frac{\bar{v}_T^2}{\Lambda^2}. \tag{2.11}$$

- Corrections due to $\mathcal{L}_8$. These corrections introduce a theoretical error

$$\Delta_{\mathcal{L}_8} \simeq \frac{\bar{v}_T^4}{\Lambda^4} \simeq \left(\frac{0.06\,(1\,\text{TeV})^2}{\Lambda^2}\right)\frac{\bar{v}_T^2}{\Lambda^2}. \tag{2.12}$$

Although it is possible to consider some corrections due to $\mathcal{L}_8$ to be absorbed into the definition of the effective parameter constrained in a measurement, using this constraint in an alternative process with different corrections due to $\mathcal{L}_8$ makes this redefinition inadvisable.

Some $\mathcal{O}(\bar{v}^4/\Lambda^4)$ terms in the χ^2 are of particular concern. Consider expanding the prediction for an observable $\bar{O}_i$ to second order

$$\bar{O}_i = O_i + \sum_{k=1}^{q_i}\left[\alpha_{i,k}C_{i,k}^6 + \sum_{l=1}^{p_i}\zeta_{i,k,l}\,C_{i,k}^6\,C_{i,l}^6\right] + \sum_{k=1}^{r_i}\gamma_{i,k}C_{i,k}^8 + \mathcal{O}\left(\frac{\bar{v}_T^6}{\Lambda^6}\right). \quad (2.13)$$

In expanding a χ^2 function, $\zeta_{i,k,l}$ terms, which exist in general at tree level[7], are the same order as the terms in a χ^2 function that dictate the global minimum for the $\mathcal{L}_6$ parameters C_i, and hence the confidence regions. These ζ terms are of power counting order $\mathcal{L}_8$ but they are potentially more problematic than new dimension eight operators for consistent fit efforts. The reason is that these terms contribute to the Hessian matrix that defines the global minimum. As the ζ terms are unknown, this matrix is formally undetermined at $\mathcal{O}(\bar{v}_T^4/\Lambda^4)$ in the χ^2, for fitting the parameters in $\mathcal{L}_6$.

- Off shell effects due to the neglect of four fermion operators when considering near Z pole LEPI data. These corrections limit the precision of bounds on parameters in $\mathcal{L}_6$ extracted from Γ_Z and $R_f^0 = \Gamma_{had}/\Gamma_{Z\to\bar{f}f}$ and are [26]

$$\Delta_{\text{offshell},\Gamma_{\text{had}}} \simeq \frac{5}{\Gamma_{had}}\frac{\Gamma_Z\hat{m}_Z}{\bar{v}_T^2}\frac{\hat{m}_Z\Gamma_Z}{24\pi^2\Gamma(Z\to\ell\bar{\ell})}\frac{\hat{m}_Z^2}{\bar{v}_T^2}\mathcal{F}\frac{\bar{v}_T^2}{\Lambda^2},$$

$$\simeq 0.4\%\frac{\bar{v}_T^2}{\Lambda^2}, \quad (2.14)$$

$$\Delta_{\text{offshell},\Gamma(Z\to f\bar{f})} \simeq \frac{N_c\Gamma_Z\hat{m}_Z}{\bar{v}_T^2}\frac{\Gamma_Z\hat{m}_Z}{12\times6\pi^2\Gamma(Z\to f\bar{f})\Gamma(Z\to\ell\bar{\ell})}\frac{\hat{m}_Z^2}{\bar{v}_T^2}\mathcal{F}\frac{\bar{v}_T^2}{\Lambda^2}, \quad (2.15)$$

$$\Delta_{\text{offshell},R_f} \simeq \Delta_{\text{offshell},\Gamma_{\text{had}}} - \Delta_{\text{offshell},\Gamma(Z\to f\bar{f})},$$

$$\simeq 0.15\%\frac{\bar{v}_T^2}{\Lambda^2},\ 0.07\%\frac{\bar{v}_T^2}{\Lambda^2},\ 0.04\%\frac{\bar{v}_T^2}{\Lambda^2}\text{ for }\ell,\text{ u, d respectively}, \quad (2.16)$$

$$\Delta_{\text{offshell},\Gamma_Z} \simeq \Delta_{\text{offshell},\Gamma_{\text{had}}} + 3\Delta_{\text{offshell},\Gamma(Z\to\ell\bar{\ell})},$$

$$\simeq 2\%\frac{\bar{v}_T^2}{\Lambda^2}. \quad (2.17)$$

Here $\mathcal{F}$ is an unknown scaling factor for the effect of these corrections in the off the Z pole LEPI data included in global analyses. This correction factor is difficult to quantify, but can be taken to be $\sim 40\,\text{pb}^{-1}/155\,\text{pb}^{-1}$ as a rough approximation. For cross section measurements this error can be neglected, see Ref [26] for a detailed discussion.

The number of operators in $\mathcal{L}_6$ and $\mathcal{L}_8$ leading to $\Delta_P, \Delta_{P,II}, \Delta_{\text{offshell},O_i}, \Delta_{\mathcal{L}_8}$ is large.[8] It is reasonable to consider these corrections added in quadrature when considering the SMEFT

---

[7]To our knowledge, these ζ terms, despite their obvious importance, have not been calculated for any observable in EWPD.

[8]The growth in the number of independent operators in considering $\mathcal{L}_6$ extended to $\mathcal{L}_8$ is expected to be (roughly) factorial, and the number of operators in $\mathcal{L}_6$ is already 59. Conversely the number of parameters in $\mathcal{L}_6$ is 2499 for the most general case, and 76 for the case where the flavour symmetry assumption we adopt is imposed [29]. The distinction between operators and parameters is due to the presence of multiplets of the symmetry groups present.

theory error metric so that $\Delta_P, \Delta_{P,II}$ multiply a further numerical factor $\sqrt{N_6}$, which is an order one number characterizing the number of $\mathcal{L}_6$ operators that contribute. We also multiply the error due to the neglect of $\mathcal{L}_8$ by an order one number $\sqrt{N_8}$ for this reason. We absorb these factors into the definition of the theoretical error.

Adding these sources of theoretical error in quadrature defines a theory error metric

$$\Delta^i_{SMEFT}(\Lambda) = \sqrt{\Delta^2_{IFI,O_i} + \Delta^2_P + \Delta^2_{P,II} + \Delta^2_{\mathcal{L}_8} + \Delta^2_{\text{offshell},O_i}}. \tag{2.18}$$

When considering detectors operating off the Z pole, the contribution from $\Delta_{\text{offshell},O_i}$ can be neglected. Generally, at low Λ the neglect of $\mathcal{L}_8$ dominates, while as Λ gets larger, the neglect of RG perturbative corrections begins to dominate. A reasonable approximation is given by

$$\Delta^i_{SMEFT}(\Lambda) \simeq \sqrt{N_8}\, x_i \, \frac{\bar{v}_T^4}{\Lambda^4} + \frac{\sqrt{N_6}\, g_2^2}{16\, \pi^2} \, y_i \, \log\left[\frac{\Lambda^2}{\bar{v}_T^2}\right] \frac{\bar{v}_T^2}{\Lambda^2}. \tag{2.19}$$

Here x_i, y_i label the observable dependence and are $\mathcal{O}(1)$. This error is multiplicative and the absolute error is obtained as $\Delta^i_{SMEFT}(\Lambda) \times O_i$. The most precise measurements at LEPI include the Z width (Γ_Z) which has a precision

$$\left(\frac{\Delta\Gamma_Z}{\Gamma_Z}\right)_{\text{Exp}} \sim 0.1\%, \qquad \left(\frac{\Delta\Gamma_Z}{\Gamma_Z}\right)_{\text{SM theory}} \sim 0.02\%. \tag{2.20}$$

Whether Δ^i_{SMEFT} is negligible, or dominant when considering an observable, depends upon the implicit assumptions about Λ adopted in a SMEFT fit, see Fig. 1. Δ^i_{SMEFT} corresponds to a theoretical error "wall" on how precisely some SMEFT corrections can be currently bounded. This is particularly the case for the most precise LEPI observables, which are per-mille constraints – *experimentally*.

It is possible in some UV scenarios that our power counting assumption essentially does not apply. We have made the simplifying choice to suppress all operators by the same scale Λ, for illustrative results, to determine in some simple cases how large an impact SMEFT theory errors have.

2.4.2 Low energy measurements

For measurements at effective scales $\mu^2 \ll \bar{v}_T^2$ it is appropriate to integrate out the Higgs, top, W, Z bosons etc. and transition to a general low(er) energy SM EFT (denoted *SMeFT*). Below the mass scales of these states the operators present in the Effective Lagrangians we will consider run according to the Renormalization group equations in the *SMeFT*, determined with no propagating states with masses $\sim \bar{v}_T$.[9] We are neglecting these running effects (as well as the threshold matching corrections) which necessitates introducing another theoretical error. These corrections lead to theoretical errors on the order of

$$\Delta_{SMeFT} \simeq \frac{g_{1,2,3}^2}{16\, \pi^2} \left(c + d \log\left(\frac{Q^2}{\hat{m}_Z^2}\right)\right) \sim 5\% \frac{\bar{v}_T^2}{\Lambda^2}, \text{ for } c = d = 1 \text{ and } Q = 0.01 \text{ GeV}, \tag{2.21}$$

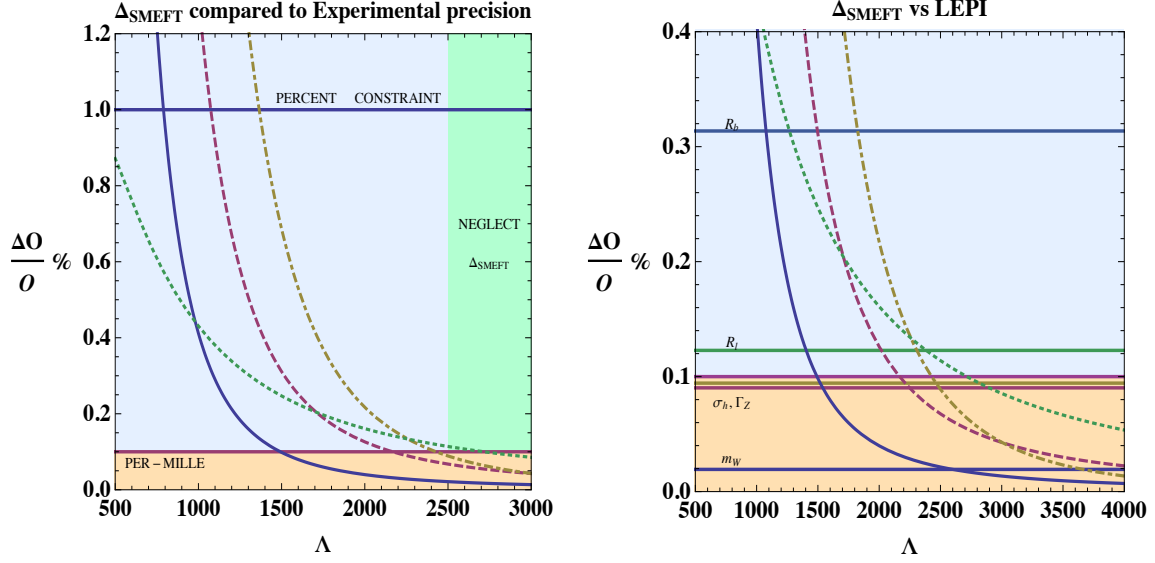[9]For an example of an analysis of this form see Ref. [43].

Figure 1. The effect of neglecting Δ_{SMEFT} on extracted constraints. $\Delta O/O$ is the experimental precision of a measurement in percent. The [solid,dashed,dot-dashed,dotted] curves correspond to $(\sqrt{N_8}\, x_i, \sqrt{N_6}\, y_i)$ values of $(1,1)$, $(\sqrt{10}, \sqrt{10})$, $(3\sqrt{10}, 0)$, $(0, 3\sqrt{10})$ in the simplified theory error metric. The left plot shows the generic impact on percent and per-mille bounds *experimentally*, while the right shows specific LEPI observables compared to theory error. The actual impact of neglected terms depends strongly on the particular UV scenario integrated out. It seems reasonable to neglect Δ^i_{SMEFT} when considering LEPI data only when very large cut off scales are implicitly assumed. The SMEFT is not currently developed to a level that allows a consistent incorporation of LEPI data if the SMEFT theory error is not included, for cut off scales $\Lambda \lesssim 3\,\text{TeV}$.

on the coefficient of the low energy operator in the Effective Lagrangian, when a low scale measurement is made at $s \sim Q^2$. Higher order terms in the expansion of $Q^2/\hat{m}_Z^2$ are neglected, with give a much smaller error $\mathcal{O}(10^{-6})$, for $Q \ll 1\,\text{GeV}$. Although the running of the lower energy operators can be incorporated directly, the resulting reduction in the theoretical error is not substantial, until $\mathcal{L}_8$ is known. This is because at the threshold when matching the linear SMEFT to the *SMeFT* at $s \sim \bar{v}_T^2$, unknown terms in SMEFT of the form $(\bar{\psi} D^\mu \psi)(\bar{\psi} D_\mu \psi)$ (for example) are present. These operators can give tree level matching corrections that are on the order of $\mathcal{O}(\bar{v}_T^2/\Lambda^2)$ to the effective operators considered in the lower energy theory. For $\Lambda \sim \text{TeV}$, the resulting theoretical errors on the effective Wilson coefficients are comparable to Δ_{SMeFT}. The situation changes once $\mathcal{L}_8$ is known, and more precise bounds can be pursued. The SMEFT error metric for low energy measurements is approximated as

$$\Delta_{SMEFT,Low} = \sqrt{(\Delta^i_{SMEFT})^2 + (\Delta_{SMeFT})^2}. \tag{2.22}$$

2.5 Impact of reducing Δ_{SMEFT}

The impact of systematically improving the SMEFT predictions, and the sensitivity of bounds on coefficients in $\mathcal{L}_6$ to theory errors is a subject of some debate in the literature currently,

following the stressing of these issues in Ref. [26]. It is subtle to correctly characterize the impact of neglected effects and theoretical errors for the following reason.

Consider the effect of changing an error in the fit when Δ_{SMEFT} becomes dominant, as in the case of some LEPI observables with a lower cut off scale. For example, consider changing the theory error on the W mass from $\Delta'_{M_W} \sim 0.2\%$ (including Δ_{SMEFT}) to $\Delta_{M_W} \sim 0.02\%$ (neglecting Δ_{SMEFT}). The later value is the quoted theory error in the SM alone. The χ^2 function constructed will then be modified with some terms obtaining corrections of the form

$$\frac{C_i^6 \, C_j^6}{(\Delta'_{M_W})^2} + \cdots = \frac{C_i^6 \, C_j^6}{100 \, \Delta_{M_W}^2} + \cdots . \tag{2.23}$$

Such changes to the most precisely measured observables do not have a negligible effect on the confidence regions obtained, see Section 3.

It is reasonable to attempt to characterize the effect of neglected higher order terms and corrections by expanding the likelihood in the correction to the observables. Then one obtains a modification of the form

$$+ 2 \sum_{i=1}^{n} \sum_{k,l=1}^{q} \sum \frac{1}{\Delta_i^2} \left[\zeta_{i,k,l} C_k^6 C_l^6 \right] \left(\hat{O} - O \right)_i + 2 \sum_{i=1}^{n} \sum_{k=1}^{r} \frac{1}{\Delta_i^2} \gamma_{i,k} C_k^8 \left(\hat{O} - O \right)_i, \tag{2.24}$$

to the χ^2 when neglecting correlations between the different observables. These effects are numerically suppressed relative to χ^2 terms of the form

$$\sim \sum_{i=1}^{n} \sum_{k=1}^{q_i} \sum_{l=1}^{q_i} \frac{C_{i,k}^6 \, C_{i,l}^6}{(\Delta_i)^2}. \tag{2.25}$$

The numerical suppression is due to the fact that $\left(\hat{O} - O \right)_i \sim \Delta_i$ so that a relative suppression by Δ_i is numerically present when considering $\zeta_{i,k,l}, \gamma_{i,k} \sim 1.$[10] This can lead to numerical behavior that indicates that these terms have a small effect on the likelihood. Studying this issue without *simultaneously* changing the theory error in the fit (i.e while neglecting the effects of the changes in Eqn. 2.23) leads to the wrong conclusion on the sensitivity of the fit to higher order effects. This error has been very frequently made in the literature.

It is important to stress that Δ_{SMEFT} can be systematically reduced, if more sophisticated theoretical predictions are developed. It is essential that a non redundant and well defined basis of $\mathcal{L}_8$ be determined.[11] Perturbative corrections to one loop order for $\mathcal{L}_6$ operators are also required to be systematically determined and included in the SMEFT, to advance the effort to reduce the (potentially) dominant theoretical errors.[12]

---

[10]This does not correspond to a power counting suppression as there is no evidence of BSM physics.

[11]This important step was reported inbetween the posting of version one and version two of this paper in Ref. [7].

[12]For recent advances in this area see Refs. [40–42, 44].

3 Numerical results

The Appendix contains details on the data and theoretical calculations used to perform the global fit. In this Section we present our results.

3.1 LEPI results

We use the systematic results in Ref. [26] for redefining the input observables in the SMEFT and making LEPI predictions. The data and theory predictions in the SM are given in Table 5. We present two results, one applicable for lower cut off scales ($\Lambda \lesssim 3\,\mathrm{TeV}$), where the error in observables that are more than percent level precise is assumed to be dominated by $\Delta_{SMEFT,i}$, and one applicable for larger cut off scales where $\Delta_{SMEFT,i}$ is neglected. In the second case, we find

$$\chi^2_{LEPI} \simeq 12.0 + \frac{10^3\,\bar{v}_T^2}{\Lambda^2} A^i C_i^{Zpole} + \frac{10^6\,\bar{v}_T^4}{\Lambda^4} (C_i^{Zpole})^T M_{ij}^{LEPI} C_j^{Zpole}, \tag{3.1}$$

where

$$A = \{7.39, -2.43, -0.270, -5.28, 3.67, 10.4, -1.23, -2.35, 4.71, 4.54\}, \tag{3.2}$$

$$C^{Zpole} = \{C_{He}, C_{Hu}, C_{Hd}, C_{Hl}^{(1)}, C_{Hl}^{(3)}, C_{Hq}^{(1)}, C_{Hq}^{(3)}, C_{ll}, C_{HWB}, C_{HD}\}, \tag{3.3}$$

and M^{LEPI} is given by

$$\begin{pmatrix}
7.53 & 0.704 & -0.253 & -7.61 & -6.02 & 0.257 & 3.95 & 0.709 & -3.98 & -0.354 \\
- & 5.91 & 2.17 & -0.814 & -3.70 & -27.9 & 1.88 & 1.65 & -3.51 & -0.826 \\
- & - & 0.99 & 0.813 & -0.302 & -11.4 & -0.414 & 0.401 & -1.38 & -0.200 \\
- & - & - & 15.7 & 4.21 & -2.5 & -6.54 & 2.85 & -4.48 & -1.43 \\
- & - & - & - & 17.2 & 10.5 & -8.44 & -7.95 & 16.9 & 6.49 \\
- & - & - & - & - & 138 & -2.22 & -6.06 & 15.9 & 3.03 \\
- & - & - & - & - & - & 7.31 & 2.43 & -2.17 & -1.22 \\
- & - & - & - & - & - & - & 5.56 & -10.6 & -4.04 \\
- & - & - & - & - & - & - & - & 28.4 & 10.2 \\
- & - & - & - & - & - & - & - & - & 4.35
\end{pmatrix}.$$

The M^{LEPI} matrix is symmetric so the lower triangular entries are not shown. For lower cut off scales ($\Lambda \lesssim 3\,\mathrm{TeV}$) we introduce a common $\Delta_{SMEFT,i} \sim \Delta$. We further approximate $\Delta \sim 0.3\%$ following the discussion in Section 2.4.1. In this case, this error will significantly affect the impact of the measurements $R_\ell, \sigma_{had}, \Gamma_Z, M_W$ on the fit space. To illustrate the impact of theory error. We find the LEPI constraint χ^2 function is

$$\chi^{2,<3\mathrm{Tev}}_{LEPI} \simeq 7.49 + \frac{10^3\,\bar{v}_T^2}{\Lambda^2} A^{i,<3} C_i^{Zpole} + \frac{10^6\,\bar{v}_T^4}{\Lambda^4} (C_i^{Zpole})^T M_{ij,<3}^{LEPI} C_j^{Zpole}, \tag{3.4}$$

where

$$A^{<3} = \{3.26, -1.26, 0.0475, 1.98, -3.57, 5.46, -0.265, 2.95, -7.40, -1.46\}, \tag{3.5}$$

and $M_{<3}^{LEPI}$ is

$$\begin{pmatrix}
2.28 & 0.142 & 0.0767 & 0.611 & -2.89 & -0.342 & -0.504 & -1.86 & -4.60 & -0.928 \\
- & 3.67 & 1.43 & -0.049 & -1.72 & -17.8 & 0.664 & 0.858 & -2.04 & -0.429 \\
- & - & 0.588 & 0.172 & -0.660 & -7.06 & 0.13 & 0.401 & -1.02 & -0.201 \\
- & - & - & 2.15 & -1.02 & -0.562 & -0.719 & 1.36 & -3.35 & -0.680 \\
- & - & - & - & 4.93 & 7.71 & -1.22 & -3.12 & 7.16 & 1.57 \\
- & - & - & - & - & 87.3 & -2.45 & -4.10 & 10.1 & 2.05 \\
- & - & - & - & - & - & 0.923 & 0.390 & -0.564 & -0.195 \\
- & - & - & - & - & - & - & 2.29 & -5.27 & -1.15 \\
- & - & - & - & - & - & - & - & 12.7 & 2.65 \\
- & - & - & - & - & - & - & - & - & 0.584
\end{pmatrix}.$$

Comparing $\chi_{LEPI}^{2,<3\text{Tev}}$ and χ_{LEPI}^{2} we see that the impact of theory error is not negligible. To further visually illustrate the impact of accounting for theoretical errors in LEPI data we take the results for χ_{LEPI}^{2} and compare the constraints for a χ^2 function developed with a varying $\Delta_{SMEFT} = \{0.3\%, 1\%\}$.

To make the comparison easy to interpret we show the dependence on a subset of Wilson coefficients. We plot the confidence regions about the χ^2 minimum setting all parameters other than those corresponding to the S, T parameters to zero. We use the normalization

$$S = \frac{16\,\pi\,\bar{v}_T^2}{g_1\,g_2}\frac{C_{HWB}}{\Lambda^2}, \qquad T = -2\,\pi\,\bar{v}_T^2\left(\frac{1}{g_1^2}+\frac{1}{g_2^2}\right)\frac{C_{HD}}{\Lambda^2}. \tag{3.6}$$

This case corresponds to a traditional oblique S, T fit in EWPD, following the formalism of Refs. [45–48]. The impact of Δ_{SMEFT} is shown in Fig. 2. The plots shown can be understood as relaxing the defining assumption of an oblique analysis, that all SMEFT parameters other than S, T vanish. This defining assumption is not RGE invariant (and challenged by field redefinitions in the SMEFT [20, 49]), so it is clearly relaxed in a more consistent analysis. We also show in the following section the effect of profiling away all other parameters other than S, T, which further increases the confidence level regions. However, the results obtained in the two cases should only be compared with caution, as they correspond to two different defining conditions for the confidence level regions.

In Fig. 3 the impact of varying Δ_{SMEFT} on the bounds of the $Z f \bar{f}$ vertex operators $C_{He}, C_{Hq}^{(3)}$ is shown. We also show the confidence levels for the two parameters C_{He} and $C_{Hq}^{(3)}$ when the remaining parameters are profiled away[13] in Fig. 5. Finally, in Table. 1 we show the 1σ confidence regions where all other parameters are profiled away.

We do not find that all individual $Z \ell \bar{\ell}$ couplings due to $\mathcal{L}_6$ (such as $C_{He}\bar{v}_T^2/\Lambda^2$) are constrained at the per-mille, or sub-per-mille level in a completely model independent fashion. If bounds on deviations are to be completely model independent when the SMEFT is assumed, then the case where Δ_{SMEFT}^{i} is dictated by a low cut off scale ($\Lambda \sim 1 - 3\,\text{TeV}$) must be

---

[13]Our profiling method is defined in the next section.
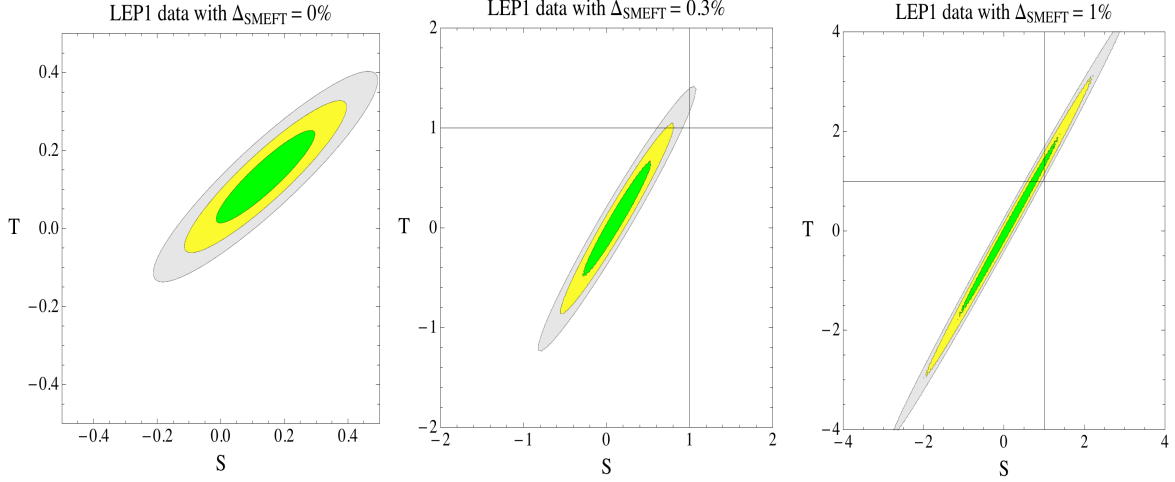
Figure 2. The effect of varying Δ_{SMEFT} on an oblique analysis. The green, yellow, grey regions correspond to the $68\%, 95\%$ and 99.9% CL regions for a two parameter fit around the minimum of the χ^2 distribution. The regions correspond to $\chi^2 = \chi^2_{min} + \Delta\chi^2$ with $\Delta\chi^2 = 2.30$ (1σ, green), 6.18 (2σ,yellow), 11.83 (3σ, grey) defined via the Cummulative Distribution function for a two parameter fit. The left plot does not include any theory error for the EFT, the middle sets $\Delta_{SMEFT} \sim 0.3\%$, the right sets $\Delta_{SMEFT} \sim 1\%$.
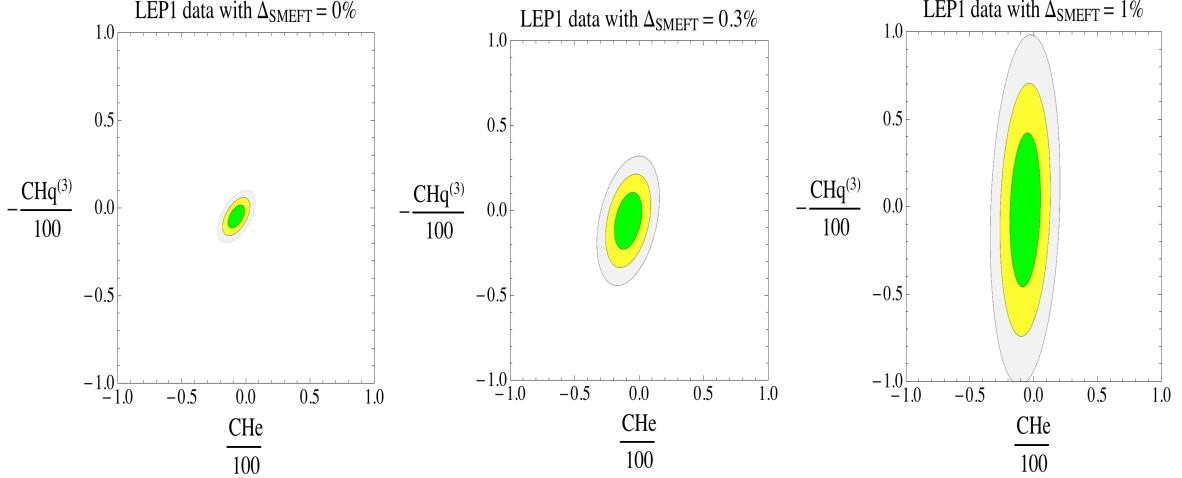
Figure 3. This figure shows directly that per-mille bounds on Z couplings (in this case $C_{He}\bar{v}_T^2/\Lambda^2$ and $C_{Hq}^{(3)}\bar{v}_T^2/\Lambda^2$) to fermions can be relaxed to $\sim \%$ constraints when considering the effect of $\Delta_{SMEFT,i}$. Conventions for the confidence regions as in the previous figure.

accommodated. As a result, the case where Δ_{SMEFT} is not negligible is always relevant for a model independent constraint. The case where the cut off scale is not too large, and patterns of deviations can be measurable, is also the case where global fits are of most interest.

The plot results shown assume that the "correct" global minimum is obtained in the χ^2 distribution when determining the confidence regions of the parameters in $\mathcal{L}_6$. There is ample

reason to expect this to not be the case, see Ref. [26] for some discussion on this point. Again we stress that the Hessian matrix that defines the global minima is formally undetermined at $\mathcal{O}(\bar{v}_T^4/\Lambda^4)$ in the χ^2 for fits to parameters in $\mathcal{L}_6$. It is important to calculate the ζ terms in the SMEFT for precisely measured observables for this reason.

3.2 Global Fit results

The global fit of all observables listed in the Appendix has nineteen Wilson coefficients

$$C_G = \frac{\bar{v}_T^2}{\Lambda^2}\{C_i^{Zpole}, C_{ee}, C_{eu}, C_{ed}, C_{\ell e}, C_{\ell u}, C_{\ell d}, C_{\ell q}^{(1)}, C_{\ell q}^{(3)}, C_{qe}\}, \tag{3.7}$$

and a total of one hundred and three observables. When considering the global analysis, $r = 17$ when our fitting assumptions[14] are adopted. Our approach to the remaining flat directions is to fix the sum of the null vectors of the fit space to their power counting size in a manner consistent with the error assigned. This introduces two auxiliary conditions on the fit that are fixed to $\bar{v}_T^2/\Lambda^2$ with $\Lambda \simeq \{4, 2, 1.5, 1.3, 1\}$TeV for $\Delta_{SMEFT} = \{0, 0.1\%, 0.3\%, 0.5\%, 1\%\}$. A simultaneous global analysis involving the observables considered here, and measurements of exclusive W pair production processes (while no parameters in the SMEFT are set to zero) is expected to fix these flat directions to a size consistent with the theoretical error determined by the power counting. In the absence of such a truly global analysis, we fix the flat directions to not be zero, but to a value consistent with their power counting size and the Δ_{SMEFT} assumed, as a reasonable approximation.

Fitting in the SM alone, with no SMEFT parameters, $\chi^2/\nu = 0.96$, where $\nu = \dim(\Omega_O) - r$. This indicates a good fit with no evidence of BSM physics. Fitting in the SMEFT (with $\Delta_{SMEFT} = 0$) changes this number to $\chi^2_{min}/\nu = 0.91$. The different values of Δ_{SMEFT} we examine modifies this goodness of fit test to $\chi^2_{min}/\nu = \{0.91, 0.90, 0.87, 0.81\}$ for the cases $\Delta_{SMEFT} = \{0.1\%, 0.3\%, 0.5\%, 1\%\}$. See Table. 1 for the χ^2_{min} value in each case.

3.3 Profiling to lower dimensional fit spaces

The constraints on each C_G^i when $C_G^{j \neq i}$ is profiled over is of some interest in building intuition on the model independent degree of constraint. However, we caution that considering constraints on individual parameters while profiling, as opposed to the constrained Eigenvectors (of the Fisher matrix) can also be misleading.

We calculate the χ^2 and express it as

$$\chi_G^2(C_G) = \chi_{G,min}^2 + (C_G - C_{G,min})^T \mathcal{I}(C_G - C_{G,min}), \tag{3.8}$$

where $C_{G,min}$ corresponds to the Wilson coefficients vector minimizing the χ_G^2 and $\mathcal{I}$ is the Fisher information matrix.

To profile away parameters $C_{G,min}^{i \notin [\![1,n]\!]}$ and retain dependence on C_G^i with $i \in [\![1,n]\!]$, we introduce the vectors $C_\perp = \{C_G^{i \notin [\![1,n]\!]}\}$ and $C_\parallel = \{C_G^{i \in [\![1,n]\!]}\}$. We then note $C_{\perp,min} = \{C_{G,min}^{i \notin [\![1,n]\!]}\}$

---

[14]$U(3)^5$ symmetry and $C_i^6 \in R$. The previous version of this manuscript reported $r = 19$ due to an error in Ref.[26] that propagated to this work.

and $C_{\parallel,min} = \{C_{G,min}^{i \in [\![1,n]\!]}\}$ so that $C_G = \{C_\perp^i, C_\parallel^i\}$ and $C_{G,min} = \{C_{\perp,min}^i, C_{\parallel,min}^i\}$. We denote by $C_{\perp,min,P}$ the vector $C_\perp$ that minimizes the χ^2 when the n parameters $C_\parallel^i$ are free. Note that $C_{\perp,min} \neq C_{\perp,min,P}$ but are related by the following formula

$$C_{\perp,min,P} = C_{\perp,min} - \mathcal{I}_\perp^{-1} \tilde{\mathcal{I}} \left(C_\parallel - C_{\parallel,min} \right), \tag{3.9}$$

where $\mathcal{I}_\perp$, $\tilde{\mathcal{I}}$ and $\mathcal{I}_\parallel$ all correspond to the components of $\mathcal{I}$ defined as

$$\mathcal{I} = \begin{pmatrix} \mathcal{I}_\perp & \tilde{\mathcal{I}} \\ \tilde{\mathcal{I}}^T & \mathcal{I}_\parallel \end{pmatrix}. \tag{3.10}$$

Calculating $C_{\perp,min,P}$ using 3.9 and using its value in $\chi_G^2 (C_G)$, we get the profiled $\chi_P^2 \left(C_\parallel \right)$ that only depends on the remaining n parameters $C_\parallel^i$. To get a constraint on one Wilson coefficient C_G^I, we profile away all other Wilson coefficients as described above taking the particular case $n = 1$. Then, using $\chi_P^2 \left(C_\parallel = C_G^I \right)$, we calculate the 1σ confidence level region for C_G^I as usual. We repeated this procedure for a SMEFT error equals to $\{0\%, 0.1\%, 0.3\%, 0.5\%, 1\%\}$ and for each value taken, we quote $\chi_{G,min}^2$, $C_{G,min} \pm \sigma$ as well as the full Fisher information matrix $\mathcal{I}$ in the Appendix. We give the $C_{G,min} \pm \sigma$ in Table 1, which shows $\mathcal{O}(\%)$ or $\mathcal{O}(10\%)$ constraints on the individual C_G^i.

Taking $n = 2$ we obtain a two parameter fit for Wilson coefficients we are interested in. We plot an nontraditional S, T result - where all others parameters than S, T are profiled away and not taken to zero - for different values of the SMEFT error: $\{0\%, 0.3\%, 1\%\}$ in Fig.4. These confidence regions should be interpreted with care. In a well defined model in the UV, a set of predictions for all the C_G^i will be present. Such a model leads to relations between the Wilson coefficients, that need to be imposed on the global fit space. Note that the global results given in the Appendix, has been minimized with respect to the C_G^i, treating the C_G^i as free parameters. The parameters profiled away can still lead to a model being excluded, even if the remaining parameters in the low energy limit of the model are consistent with the confidence regions shown in Fig. 4,5. This is due to the fact that these confidence regions are valid when the parameters profiled away are treated as free. Further, we note that the S, T result in Fig. 4 should only be compared with caution to Fig. 2, due to the different assumptions employed in the analyses. Nevertheless, it is still interesting that relaxing the strict assumptions of an oblique analysis (that all parameters other than S, T are neglected) will generally lead to a degree of constraint that is in between the constraints shown in Fig. 2 and Fig. 4. We also follow this procedure for the two parameters C_{He} and $C_{Hq}^{(3)}$ to compare with Fig. 3 and find the result in Fig. 5. However, we note again that this comparison requires significant caution in interpretation.

3.4   The Eigensystem of the Global Fit

The degree of constraint on orthogonal linear independent combinations of the Wilson coefficients (denoted $W_k^{\Delta_{SMEFT}}$) significantly varies for the global fit. Here $k = 1..19$ sums
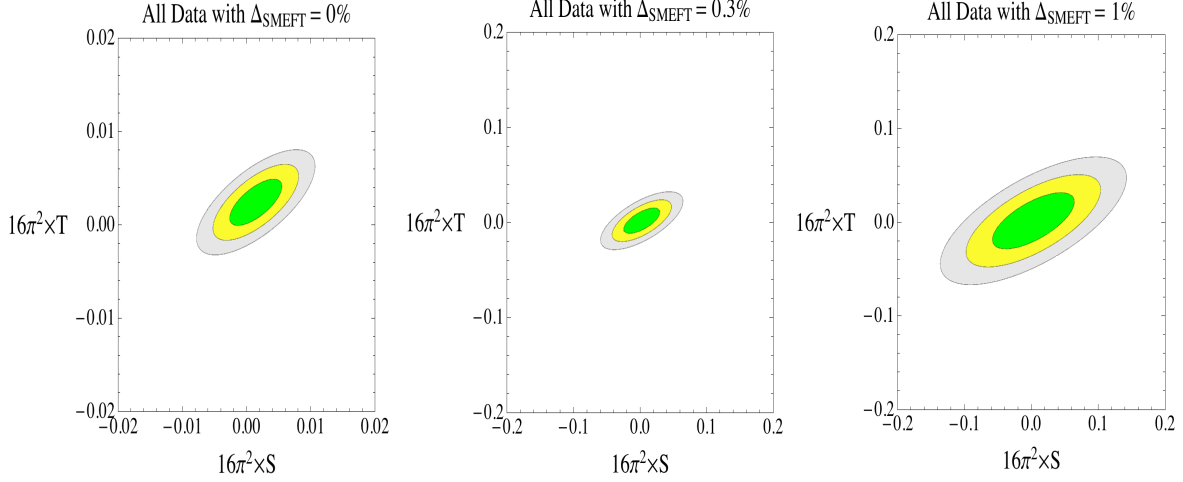
Figure 4. The effect of varying Δ_{SMEFT} on an oblique analysis, when the remaining parameters are profiled over and not set to zero. Constraints are relaxed essentially by a loop factor $\sim 16\pi^2$. Conventions for the confidence regions as in the previous figures. The interpretation of this result requires some care, see the text. We stress that this figure should not be interpreted as directly comparable to Fig. 2 as the assumptions of the two analyses fundamentally differ.
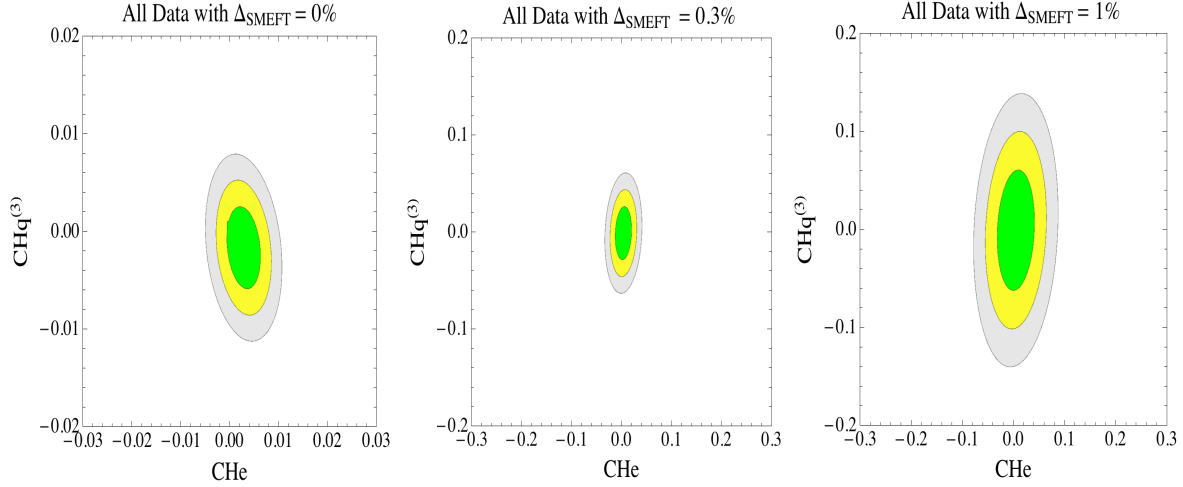
Figure 5. The fit space for $C_{He}\bar{v}_T^2/\Lambda^2$ and $C_{Hq}^{(3)}\bar{v}_T^2/\Lambda^2$ when the remaining parameters are profiled away. Conventions for the confidence regions as in the previous figures. Note the impact of profiling on the correlations in this case.

over all of the orthogonal eigenvectors (of the Fisher matrix $\mathcal{I}$) in our global fit. The normalized Eigenvectors and Eigenvalues of the system are directly obtained from the Fisher matricies given in the Appendix. The Eigenvectors are normalized so that $\sqrt{\sum_{i=1}^{19}(w_k^i)^2} = 1$ where $W_k^{\Delta_{SMEFT}} = \sum_{i=1}^{19} w_k^i C_G^i$. A particular model is present in the UV, dictating the Wilson

C_i^G	$(1\sigma, 0)$	$(1\sigma, 0.1\%)$	$(1\sigma, 0.3\%)$	$(1\sigma, 0.5\%)$	$(1\sigma, 1\%)$
χ^2_{min}	77	77	76	74	69
$\tilde{C}_{He}$	0.29 ± 0.23	0.32 ± 0.62	0.39 ± 1.1	0.44 ± 1.4	0.48 ± 2.4
$\tilde{C}_{Hu}$	0.86 ± 0.8	0.84 ± 0.88	0.81 ± 1.1	0.79 ± 1.2	0.79 ± 1.8
$\tilde{C}_{Hd}$	-3.3 ± 1.3	-3.3 ± 1.3	-3.3 ± 1.4	-3.2 ± 1.5	0.34 ± 1.2
$\tilde{C}_{Hl}^{(1)}$	0.22 ± 0.12	0.25 ± 0.32	0.31 ± 0.57	0.34 ± 0.76	0.2 ± 4.1
$\tilde{C}_{Hl}^{(3)}$	0.22 ± 0.29	0.22 ± 1	0.22 ± 1.8	0.21 ± 2.4	-0.14 ± 0.44
$\tilde{C}_{Hq}^{(1)}$	-0.12 ± 0.17	-0.13 ± 0.19	-0.13 ± 0.24	-0.14 ± 0.29	-0.08 ± 4.1
$\tilde{C}_{Hq}^{(3)}$	-0.17 ± 0.28	-0.15 ± 1	-0.12 ± 1.8	-0.09 ± 2.4	-0.01 ± 0.27
$\tilde{C}_{ll}$	-0.11 ± 0.15	-0.06 ± 0.2	-0.01 ± 0.24	-0.01 ± 0.26	0.22 ± 2.9
$\tilde{C}_{HWB}$	0.1 ± 0.19	0.13 ± 0.73	0.18 ± 1.3	0.21 ± 1.7	-0.36 ± 4.7
$\tilde{C}_{HD}$	-0.58 ± 0.39	-0.53 ± 1.2	-0.44 ± 2.1	-0.39 ± 2.8	-0.02 ± 0.36
$\tilde{C}_{ee}$	0.006 ± 0.28	-0.02 ± 0.3	-0.05 ± 0.32	-0.04 ± 0.33	-21 ± 26
$\tilde{C}_{eu}$	-27 ± 24	-26 ± 24	-24 ± 24	-22 ± 25	-21 ± 31
$\tilde{C}_{ed}$	-27 ± 30	-26 ± 31	-24 ± 31	-23 ± 31	-21 ± 31
$\tilde{C}_{\ell e}$	-0.01 ± 0.3	-0.01 ± 0.3	-0.01 ± 0.31	-0.01 ± 0.31	0.001 ± 0.32
$\tilde{C}_{\ell u}$	-17 ± 8.5	-17 ± 8.5	-17 ± 8.6	-17 ± 8.6	-17 ± 8.9
$\tilde{C}_{\ell d}$	-32 ± 16	-32 ± 16	-32 ± 16	-32 ± 16	-31 ± 17
$\tilde{C}_{\ell q}^{(1)}$	-4 ± 1.9	-3.5 ± 2.5	-2.4 ± 3.8	-1.7 ± 5	-1.3 ± 7.2
$\tilde{C}_{\ell q}^{(3)}$	-0.49 ± 0.23	-0.43 ± 0.28	-0.33 ± 0.36	-0.28 ± 0.43	-0.18 ± 0.61
$\tilde{C}_{qe}$	-1.5 ± 26	-1.9 ± 26	-2.5 ± 26	-2.9 ± 26	-4 ± 27

Table 1. Shown are the best fit points of the C_G^i and the one sigma error as a function of Δ_{SMEFT}. Here we have profiled over all $C_G^{j \neq i}$ to reduce to a one dimensional fit space. The columns are labeled as $(1\sigma, \Delta_{SMEFT})$. The Wilson coefficients have been scaled as $\tilde{C}_G^i = 100\, C_G^i$ where C_G^i contains an implicit factor $\bar{v}_T^2/\Lambda^2$. As expected the consistent introduction of a theoretical error does relax the bounds on the C_G^i. Note that even when $\Delta_{SMEFT} = 0$, individual operators that contribute to $\delta(Z\bar{\ell}\ell)$ are only model independently constrained at the percent level. Constraints on some four fermion operators are an order of magnitude weaker for the data considered.

coefficients, so in general the Eigenvectors will not have a norm of one. The inverse of the Fisher matrix is exactly the covariance matrix of the Wilson coefficients in our case, since the observables receive a linear shift in the Wilson coefficients. Diagonalizing the covariance matrix and taking its square root gives the one sigma range σ_k on the $W_k^{\Delta_{SMEFT}}$.
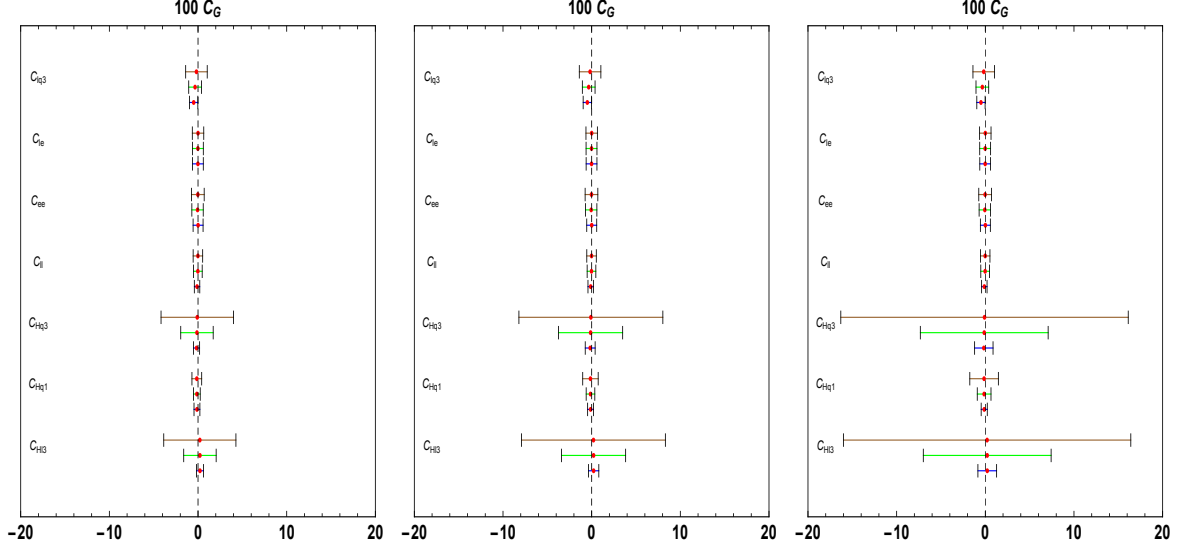
Figure 6. Represented are the $(\tilde{C}_G^i)_{min} \pm 2\sigma$ where $\tilde{C}_G^i = 100 C_G^i$. The bands are $\Delta_{SMEFT} = 1\%, 0.3\%, 0\%$ for the brown, green and blue lines respectively. We show results left to right for fixing the auxiliary constraint lifting the two flat directions to $\bar{v}_T^2/2\Lambda^2$, $\bar{v}_T^2/\Lambda^2$ and $2\bar{v}_T^2/\Lambda^2$.
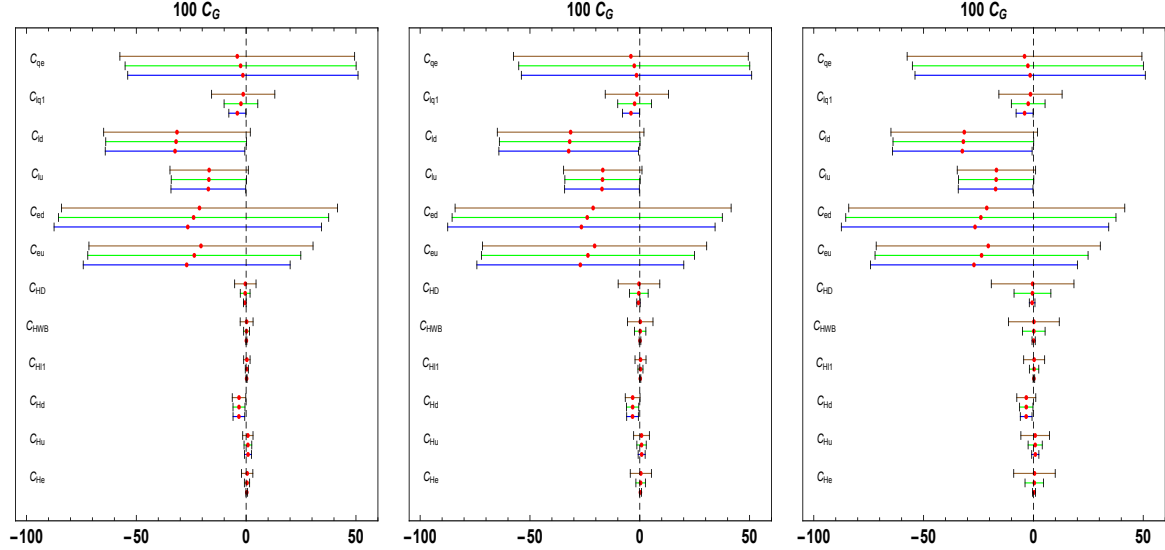
Figure 7. Represented are the $(\tilde{C}_G^i)_{min} \pm 2\sigma$ where $\tilde{C}_G^i = 100 C_G^i$. The bands are $\Delta_{SMEFT} = 1\%, 0.3\%, 0\%$ for the brown, green and blue lines respectively. We show results left to right for fixing the auxiliary constraint lifting the two flat directions to $\bar{v}_T^2/2\Lambda^2$, $\bar{v}_T^2/\Lambda^2$ and $2\bar{v}_T^2/\Lambda^2$.

We report the values $v/\sqrt{\sigma_k}$ for each W_k for $\Delta_{SMEFT} = \{0\,\%, 0.1\,\%, 0.3\,\%, 0.5\,\%, 1\,\%\}$

$$\{27, 23, 18, 17, 11, 9.6, 6.7, 5.5, 4.9, 4.4, 4.1, 4.0, 4.0, 2.9, 2.2, 1.9, 1.5, 0.54, 0.36\}_{0\%},$$
$$\{27, 18, 15, 13, 10, 6.6, 6.1, 5.5, 4.7, 4.4, 3.5, 2.8, 2.2, 2.0, 2.0, 1.8, 1.4, 0.54, 0.36\}_{0.1\%},$$
$$\{24, 17, 11, 10, 8.3, 5.8, 5.4, 5.2, 4.5, 4.2, 3.2, 2.6, 2.2, 1.8, 1.5, 1.5, 1.1, 0.54, 0.36\}_{0.3\%},$$
$$\{22, 17, 9.88.6, 7.2, 5.5, 5.2, 4.8, 4.4, 4.0, 3.1, 2.4, 2.1, 1.8, 1.3, 1.3, 0.98, 0.54, 0.36\}_{0.5\%},$$
$$\{19, 16, 9.4, 6.7, 6.2, 5.3, 4.6, 4.4, 4.0, 3.9, 5.0, 2.2, 1.8, 1.8, 1.0, 1.0, 0.82, 0.53, 0.36\}_{1\%}.$$

$$(3.11)$$
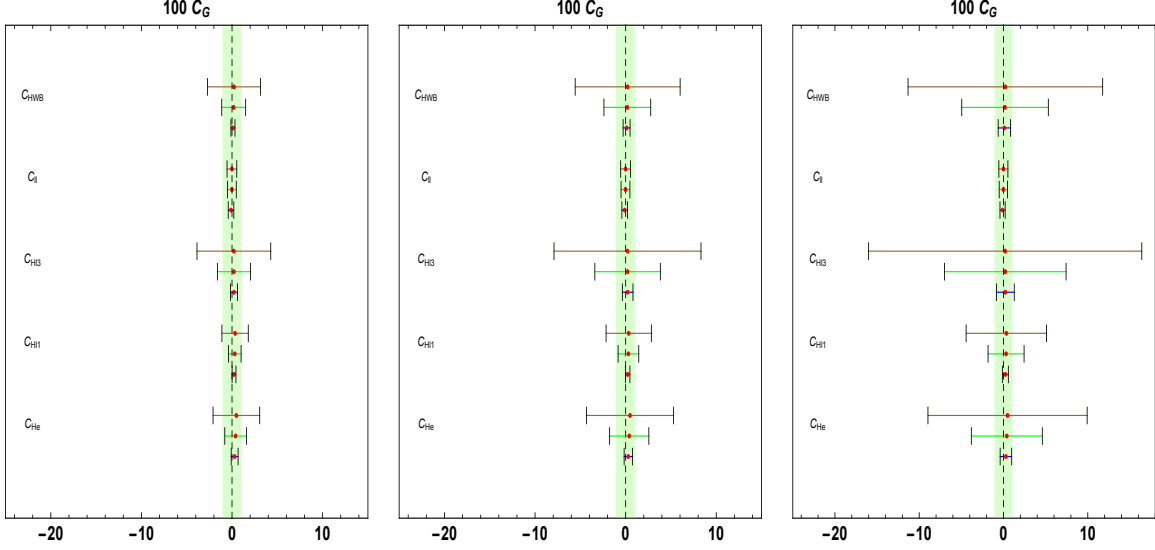
Figure 8. Here, the focus is on the Wilson coefficients contributing to the $Z\ell\bar{\ell}$ coupling redefinition. We show how the SMEFT error affects the constraints on these Wilson coefficients. The green band corresponds to having C_G^i constrained to a per mill level $< 1\%$. We show results left to right for fixing the auxiliary constraint lifting the two flat directions to $\bar{v}_T^2/2\Lambda^2$, $\bar{v}_T^2/\Lambda^2$ and $2\bar{v}_T^2/\Lambda^2$.

As $v/\sqrt{\sigma_k} < \Lambda/||W_k - W_{k,min}||$ (at one sigma) we have information on the corresponding scale of suppression (in TeV units). The scale of suppression is distinct from the cut off scale. The results show that the hierarchy of constraints is roughly dictated by LEPI observables, as expected, and these constraints are also relaxed when theory error is consistently included. Small changes in theory errors can have a dramatic impact on the most constrained Eigenvectors; for example, they change the scale of suppression on the most constrained Eigenvector by $8\,\text{TeV}$. There are six individual Wilson coefficients that effectively lead to anomalous couplings of the form $\delta(Z^\mu\,\bar{\ell}\,\gamma_\mu\,\ell)$: $C_{HWB}, C_{HD}, C_{\ell\ell}, C_{He}, C_{H\ell}^{(1)}, C_{H\ell}^{(3)}$. The six most constrained Eigenvectors do not only involve these parameters in a numerically dominant fashion, as we have explicitly verified. This can be directly checked by using the Fisher matricies supplied in the Appendix. This is the case if Δ_{SMEFT} is neglected, or not.

The most strongly constrained Eigenvector is (approximately)

$$W_1^0 \approx \pm \frac{1}{5}\left(-0.97\,C_{Hu} + 0.7\,C_{Hl}^{(3)} + 4.7\,C_{Hq}^{(1)} + 0.82\,C_{HWB} - 0.45\,C_{ll}\right)\frac{\bar{v}_T^2}{\Lambda^2}. \qquad (3.12)$$

This (approximate) Eigenvector remains constrained as Δ_{SMEFT} is not neglected, for example

$$W_1^{0.5\%} \approx \pm \frac{1}{5}\left(-0.97\,C_{Hu} + 0.56\,C_{Hl}^{(3)} + 4.8\,C_{Hq}^{(1)} + 0.78\,C_{HWB} - 0.33\,C_{ll}\right)\frac{\bar{v}_T^2}{\Lambda^2}. \qquad (3.13)$$

It is easy to understand the appearance of $C_{Hq}^{(1)}$, which gives contribution to the Z coupling to quarks, in the most constrained Eigenvector. LEPI data on the partial widths are inferred
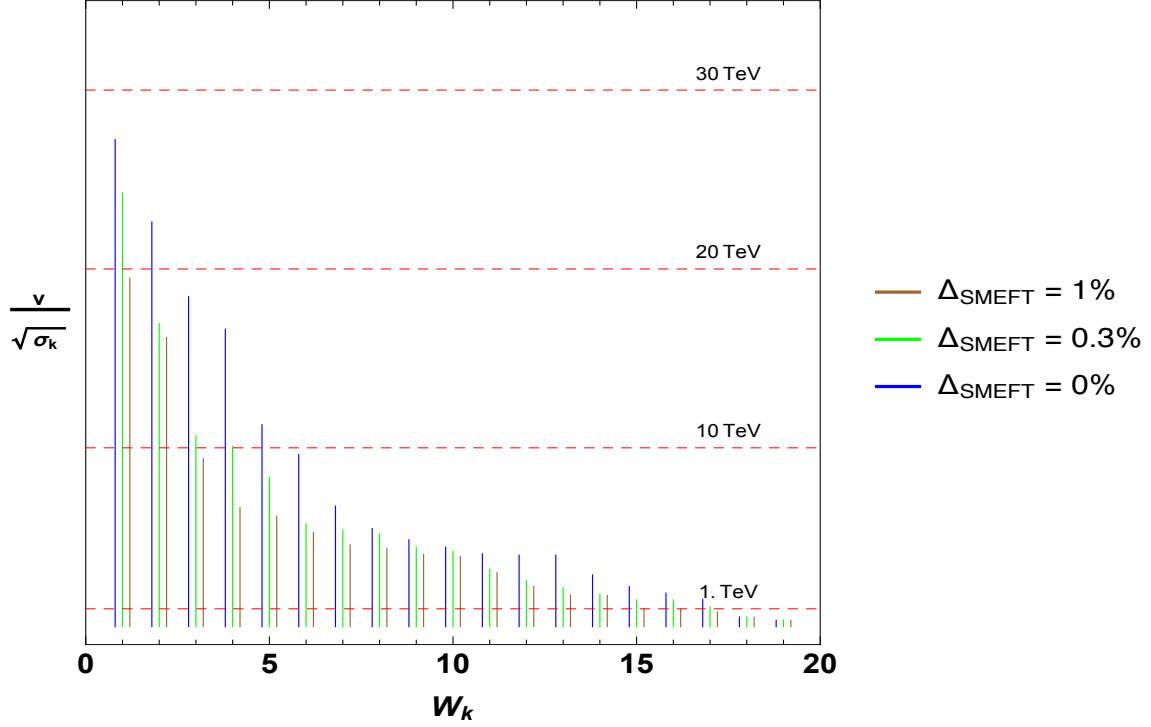
Figure 9. The values $v/\sqrt{\sigma_k}$ for each W_k for $\Delta_{SMEFT} = \{0\%, 0.3\%, 1\%\}$.

from the measurements of the pseudo-observable ratio R_f^0, that always involve the couplings of the Z to quarks.

It is reasonable to impose the global fit constraints for pre-LHC data on LHC studies, when considering possible deviations allowed in the SMEFT.[15] For example, when the effective scale in an experiment is $\mu \sim \hat{m}_Z$ the Eigenvector W_1 is highly constrained.[16] This is not equivalent to just setting $\delta(Z^\mu \, \bar{\ell} \, \gamma_\mu \, \ell) = 0$.

To optimally incorporate the constrains from global fits that include more pre-LHC data, or LHC data from Run1, this point still holds. The Eigenvectors and Eigenvalues of the system are sensitive to the full set of measurements that are required to fully constrain the Wilson coefficient space model independently.

4   Conclusions

We have developed the global constraints of the SMEFT considering data from many (pre-LHC) experiments. We have also developed a theory error metric, and used this result in

---

[15]It is also manifestly of interest to formulate joint analysis where all of the data is fit simultaneously. Note also that the quoted Fisher matricies will also be modified by the inclusion of LHC data in a joint fit.

[16]The requirement that the scale be $\mu \sim \hat{m}_Z$ is due to the fact that the Eigenvector is not preserved under RG evolution.

the global fit. We believe our results demonstrate that SMEFT theory errors should not be neglected in future fit efforts.

Our conclusions differ somewhat from recent claims in the literature. We find that the per-mille/few percent constraint hierarchy concerning experimental precision at LEPI and LEPII/LHC does not consistently translate into a hierarchy of constraints on individual leading Wilson coefficients in the SMEFT. Due to this, we stress again that, it is in our view not justified to set individual Wilson coefficients to zero in LHC analyses to attempt to incorporate pre-LHC data in the SMEFT. This is the case even before SMEFT theoretical errors are included. When these errors are added, this point is only strengthened.

Relaxing bounds on a number of unknown parameters in a global fit from the per-mille level to the few percent level is more significant than naively expected. This is because exactly this hierarchy of constraints has been used to neglect parameters in other LHC studies using the SMEFT. Inconsistent approaches to the linear SMEFT could in time lead to an incorrect conclusion that the linear SMEFT has to be abandoned, in favour of the more general nonlinear formulation. As such, obtaining precise, consistent, and reproducible bounds on the SMEFT is essential.

The differences in fit methodology, observables used, SM theoretical predictions, and our treatment of theoretical errors explains why our conclusions differ from past results. We have supplied significant details on our results to make our conclusions reproducible. These details are presented in the Appendix. We will supply the main result of the global fit likelihood (as a function of the cut off scale) in a mathematica file, upon request, to aid in reproducing our results.

Acknowledgements

V3 changes: As we aim for this fit methodology and result to be reproducible and transparent, here we list the main changes in the paper and numerics from version two to version three.

- We have corrected an error that propogated in to this work from Ref. [26] in Appendix A. This has lead to the introduction of auxiliary conditions to lift flat directions in

a manner that is dictated by the power counting of the SMEFT, consistent with the theoretical errors assigned.

- We have clarified the discussion in Section C.1 and corrected a shift related to this clarification in the fit program.

- We have updated and extended the numerics to make clear the strong dependence on the fit space of fixing the flat directions.

A   Core shifts of parameters due to the SMEFT

We use the systematic results in Ref. [26] for redefining the input observables in the SMEFT and making LEPI predictions and for $\ell^+ \ell^- \to f \bar{f}$ scattering in the SMEFT away from the Z pole. Here f is defined to be $f = \{\mu, \tau, u, c, t, d, s, b\}$ for $e^\pm$ initial states. The results we report are expressed in terms of some core shift of parameters present in the SMEFT. We include these core shifts below for completeness. Our notational conventions are that shifts due to the SMEFT are denoted as δX for a parameter X. For more details on our notation and the redefinition of the input parameters to make predictions in the SMEFT, see Ref. [26]. Measured input observables are denoted with hat superscripts. We also include the definition of the operator basis we use [4] in this Appendix for completeness.

$$\delta M_Z^2 \equiv \frac{1}{2\sqrt{2}} \frac{\hat{m}_Z^2}{\hat{G}_F} C_{HD} + \frac{2^{1/4}\sqrt{\pi}\sqrt{\hat{\alpha}}\,\hat{m}_Z}{\hat{G}_F^{3/2}} C_{HWB}, \tag{A.1}$$

$$\delta M_W^2 = -\hat{m}_W^2 \left(\frac{\delta s_{\hat{\theta}}^2}{s_{\hat{\theta}}^2} + \frac{c_{\hat{\theta}}}{s_{\hat{\theta}}\sqrt{2}\hat{G}_F} C_{HWB} + \sqrt{2}\delta G_F \right), \tag{A.2}$$

$$\delta G_F = \frac{1}{\sqrt{2}\,\hat{G}_F} \left(\sqrt{2}\, C_{Hl}^{(3)} - \frac{C_{ll}}{\sqrt{2}} \right), \tag{A.3}$$

$$\delta s_{\theta}^2 = -\frac{s_{\hat{\theta}}\, c_{\hat{\theta}}}{2\sqrt{2}\,\hat{G}_F(1 - 2s_{\hat{\theta}}^2)} \left[s_{\hat{\theta}}\, c_{\hat{\theta}}\, (C_{HD} + 4\, C_{H\ell}^{(3)} - 2\, C_{ll}) + 2\, C_{HWB} \right], \tag{A.4}$$

$$\delta(g_V^\ell)_{pr} = \delta\bar{g}_Z\, (g_V^\ell)_{pr}^{SM} - \frac{1}{4\sqrt{2}\hat{G}_F} \left(C_{He}_{pr} + C_{H\ell}^{(1)}_{pr} + C_{H\ell}^{(3)}_{pr} \right) - \delta s_\theta^2, \tag{A.5}$$

$$\delta(g_A^\ell)_{pr} = \delta\bar{g}_Z\, (g_A^\ell)_{pr}^{SM} + \frac{1}{4\sqrt{2}\,\hat{G}_F} \left(C_{He}_{pr} - C_{H\ell}^{(1)}_{pr} - C_{H\ell}^{(3)}_{pr} \right), \tag{A.6}$$

$$\delta(g_V^\nu)_{pr} = \delta\bar{g}_Z\, (g_V^\nu)_{pr}^{SM} - \frac{1}{4\sqrt{2}\,\hat{G}_F} \left(C_{H\ell}^{(1)}_{pr} - C_{H\ell}^{(3)}_{pr} \right), \tag{A.7}$$

$$\delta(g_A^\nu)_{pr} = \delta\bar{g}_Z\, (g_A^\nu)_{pr}^{SM} - \frac{1}{4\sqrt{2}\,\hat{G}_F} \left(C_{H\ell}^{(1)}_{pr} - C_{H\ell}^{(3)}_{pr} \right), \tag{A.8}$$

$$\delta(g_V^u)_{pr} = \delta\bar{g}_Z\,(g_V^u)_{pr}^{SM} + \frac{1}{4\sqrt{2}\,\hat{G}_F}\left(-C^{(1)}_{\substack{Hq\\pr}} + C^{(3)}_{\substack{Hq\\pr}} - C_{\substack{Hu\\pr}}\right) + \frac{2}{3}\delta s_\theta^2, \tag{A.9}$$

$$\delta(g_A^u)_{pr} = \delta\bar{g}_Z\,(g_A^u)_{pr}^{SM} - \frac{1}{4\sqrt{2}\,\hat{G}_F}\left(C^{(1)}_{\substack{Hq\\pr}} - C^{(3)}_{\substack{Hq\\pr}} - C_{\substack{Hu\\pr}}\right), \tag{A.10}$$

$$\delta(g_V^d)_{pr} = \delta\bar{g}_Z\,(g_V^d)_{pr}^{SM} - \frac{1}{4\sqrt{2}\,\hat{G}_F}\left(C^{(1)}_{\substack{Hq\\pr}} + C^{(3)}_{\substack{Hq\\pr}} + C_{\substack{Hd\\pr}}\right) - \frac{1}{3}\delta s_\theta^2, \tag{A.11}$$

$$\delta(g_A^d)_{pr} = \delta\bar{g}_Z\,(g_A^d)_{pr}^{SM} + \frac{1}{4\sqrt{2}\,\hat{G}_F}\left(-C^{(1)}_{\substack{Hq\\pr}} - C^{(3)}_{\substack{Hq\\pr}} + C_{\substack{Hd\\pr}}\right), \tag{A.12}$$

where

$$\delta\bar{g}_Z = -\frac{\delta G_F}{\sqrt{2}} - \frac{\delta M_Z^2}{2\hat{m}_Z^2} + \frac{s_{\hat\theta}\,c_{\hat\theta}}{\sqrt{2}\hat{G}_F}C_{HWB}, \tag{A.13}$$

and

$$\delta(g_V^{W^{\pm},\ell})_{rr} = \delta(g_A^{W^{\pm},\ell})_{rr} = \frac{1}{2\sqrt{2}\hat{G}_F}\left(C^{(3)}_{\substack{H\ell\\rr}} + \frac{1}{2}\frac{c_{\hat\theta}}{s_{\hat\theta}}C_{HWB}\right) + \frac{1}{4}\frac{\delta s_\theta^2}{s_{\hat\theta}^2}, \tag{A.14}$$

$$\delta(g_V^{W^{\pm},q})_{rr} = \delta(g_A^{W^{\pm},q})_{rr} = \frac{1}{2\sqrt{2}\hat{G}_F}\left(C^{(3)}_{\substack{Hq\\rr}} + \frac{1}{2}\frac{c_{\hat\theta}}{s_{\hat\theta}}C_{HWB}\right) + \frac{1}{4}\frac{\delta s_\theta^2}{s_{\hat\theta}^2}. \tag{A.15}$$

Here our chosen normalization is $(g_V^x)^{SM} = T_3/2 - Q^x\,\bar{s}_\theta^2$, $(g_A^x)^{SM} = T_3/2$ where $T_3 = 1/2$ for u_i, ν_i and $T_3 = -1/2$ for d_i, ℓ_i and $Q^x = \{-1, 2/3, -1/3\}$ for $x = \{\ell, u, d\}$.

B $2 \to 2$ scattering observables at LEP, Tristan, Pep, Petra.

B.1 $\ell^+\ell^- \to f\bar{f}$ near and far from the Z pole.

With the simplifying assumptions of total U(5)^5 symmetry in the effects of $\mathcal{L}_6$, real wilson coefficients and a narrow width approximation for the shifts (neglecting terms or order Γ_Z/v in the shifts, but not the error $\Delta_{SMEFT,i}$), we find the result for differential $\ell^+\ell^- \to f\bar{f}$ scattering

$$\delta\left(\frac{d\sigma_{e^+e^-\to f\bar{f}}}{d\cos(\theta)}\right) = 2\left(\frac{s\,F_1^{\ell f}}{P(s)}\right)\hat{G}_F^2\,N_c\,N_{VA}^{\ell f}\left(1 + \cos(\theta)^2\right) + \left(\frac{s\,F_2^{\ell f}}{P(s)}\right)\hat{G}_F^2\,N_c\,N_{VA}^{\ell f}\cos(\theta), \tag{B.1}$$

where we used

$$F_1^{\ell f} = \delta C_{\psi^4}^{ef+} + \frac{\left[G_A^f\,G_V^f\,G_{VA}^f\,\delta G_{VAAV}^\ell + (\ell \leftrightarrow f)\right]}{P(s)} + \frac{Q_\ell Q_f\hat{\alpha}}{s\hat{G}_F\sqrt{2}N_{VA}^{\ell f}}\left(\delta g_V^\ell G_V^f + G_V^\ell\delta g_V^f\right),$$

$$F_2^{\ell f} = 4\,\delta C_{\psi^4}^{ef-} - \frac{8}{P(s)}\left[\delta G_{VVAA}^\ell + (\ell \leftrightarrow f)\right] + \frac{4Q_\ell Q_f\hat{\alpha}}{\sqrt{2}\hat{G}_F s N_{VA}^{\ell f}}\left(\delta g_A^\ell G_A^f + \delta g_A^f G_A^\ell\right), \tag{B.2}$$

Obs.	$\sqrt{s}$	Exp. Value	Ref.	SM Value	Ref.
$f = \mu$	207	$2.618 \pm 0.078 \pm 0.014$	[51]	2.62 ± 0.0139	[52]
	205	$2.464 \pm 0.098 \pm 0.015$	[51]	2.67 ± 0.0142	[52]
	202	$2.709 \pm 0.146 \pm 0.017$	[51]	2.76 ± 0.0146	[52]
	200	$3.072 \pm 0.108 \pm 0.018$	[51]	2.82 ± 0.0149	[52]
	196	$2.994 \pm 0.110 \pm 0.018$	[51]	2.96 ± 0.0157	[52]
	192	$2.926 \pm 0.181 \pm 0.018$	[51]	3.10 ± 0.0164	[52]
	189	$3.150 \pm 0.075 \pm 0.016$	[51]	3.21 ± 0.0170	[52]
	183	$3.505 \pm 0.145 \pm 0.042$	[51]	3.46 ± 0.0183	[52]
	172	$3.562 \pm 0.331 \pm 0.058$	[51]	4.01 ± 0.0213	[52]
	161	$4.580 \pm 0.376 \pm 0.062$	[51]	4.73 ± 0.0251	[52]
	136	$9.020 \pm 0.944 \pm 0.175$	[51]	7.35 ± 0.0390	[52]
	130	$8.606 \pm 0.699 \pm 0.131$	[51]	8.51 ± 0.0451	[52]
	57.8	$27.54 \pm 0.65 \pm 0.95$	[53]	$27.42 \times (1 \pm 1\%)^{\star}$	[53]
	57.77	17.86 ± 0.35	[54]	$18.10 \times (1 \pm 1\%)^{\star}$	[54]
	35	$69.79 \pm 1.35 \pm 1.40$	[55]	$70.9 \times (1 \pm 1\%)^{\star}$	[55]
$R_{\mu\mu}^{exp/th}$	29	0.994 ± 0.022	[56]	1	

Table 2. Experimental and theoretical values of the $\sigma_{e^+e^- \to f\bar{f}}$ in pb. Note that $R_{\ell\ell}^{exp/th}$ is the quoted ratio of the experimental cross section with the SM theoretical prediction from Ref. [56, 57]. Theoretical errors are included in the quoted error for this ratio. When we construct theoretical predictions using ZFITTER, we follow the guidance of Ref. [51] and use the input observable values quoted in Ref.[26]. We discuss our approach to theoretical errors, including errors for the SMEFT theoretical framework itself, in Section 2.

with

$$
\delta C_{\psi^4}^{e\,\ell\pm} = \frac{\left[C_{ee}(G_V^\ell - G_A^\ell)^2 + C_{\ell\ell}(G_V^\ell + G_A^\ell)^2 + C_{\ell e}(G_V^\ell + G_A^\ell)(G_V^\ell - G_A^\ell)\right]}{16\sqrt{2}\pi\,\hat{G}_F\,N_{VA}^{\ell\ell}},
$$

$$
+ \frac{\hat{\alpha}P(s)}{32s\hat{G}_F^2 N_{VA}^{\ell\ell}}\left(C_{\ell\ell} + C_{ee} \pm C_{\ell e}\right), \tag{B.3}
$$

$$
\delta C_{\psi^4}^{e\,u\pm} = \frac{\left[C_{\ell u}(G_V^\ell + G_A^\ell)(G_V^u - G_A^u) + C_{eu}(G_V^\ell - G_A^\ell)(G_V^u - G_A^u)\right]}{16\sqrt{2}\pi\,\hat{G}_F\,N_{VA}^{\ell u}},
$$

$$
+ \frac{\left(C_{\ell q}^{(1)} - C_{\ell q}^{(3)}\right)(G_V^\ell + G_A^\ell)(G_V^u + G_A^u)}{16\sqrt{2}\pi\,\hat{G}_F\,N_{VA}^{\ell u}} - \frac{2\hat{\alpha}P(s)\left(\pm C_{\ell u} + C_{eu} + C_{\ell q}^{(1)} - C_{\ell q}^{(3)}\right)}{96s\hat{G}_F^2 N_{VA}^{\ell u}}, \tag{B.4}
$$

Obs.	$\sqrt{s}$	Exp. Value	Ref.	SM Value	Ref.
$f = \tau$	207	$2.502 \pm 0.109 \pm 0.029$	[51]	2.62 ± 0.0160	[52]
	205	$2.783 \pm 0.149 \pm 0.028$	[51]	2.67 ± 0.0163	[52]
	202	$2.838 \pm 0.208 \pm 0.022$	[51]	2.76 ± 0.0168	[52]
	200	$2.952 \pm 0.148 \pm 0.029$	[51]	2.82 ± 0.0172	[52]
	196	$2.961 \pm 0.152 \pm 0.029$	[51]	2.96 ± 0.0181	[52]
	192	$2.860 \pm 0.246 \pm 0.032$	[51]	3.10 ± 0.0189	[52]
	189	$3.204 \pm 0.107 \pm 0.032$	[51]	3.21 ± 0.0196	[52]
	183	$3.367 \pm 0.174 \pm 0.049$	[51]	3.46 ± 0.0211	[52]
	172	$4.053 \pm 0.469 \pm 0.092$	[51]	4.01 ± 0.0245	[52]
	161	$5.715 \pm 0.553 \pm 0.139$	[51]	4.73 ± 0.0289	[52]
	136	$7.167 \pm 0.851 \pm 0.143$	[51]	7.35 ± 0.0448	[52]
	130	$9.020 \pm 0.944 \pm 0.175$	[51]	8.51 ± 0.0519	[52]
	57.8	$28.27 \pm 0.87 \pm 0.69$	[53]	$27.42 \times (1 \pm 1\%)^{\star}$	[53]
	57.77	$17.38 \pm 0.40 \pm 0.27 \pm 0.14$	[58]	$18.10 \times (1 \pm 1\%)^{\star}$	[54]
	35	$71.72 \pm 1.48 \pm 1.61$	[55]	$70.9 \times (1 \pm 1\%)^{\star}$	[55]
$R_{\tau\tau}^{exp/th}$	29	$1.044 \pm 0.14 \pm 0.030$	[57]	1	

Table 3. Experimental and theoretical values of the $\sigma_{e^+e^- \to f\bar{f}}$ in pb.

$$\delta C_{\psi^4}^{e\,d\pm} = \frac{\left[C_{\ell d}(G_V^{\ell} + G_A^{\ell})(G_V^d - G_A^d) + C_{ed}(G_V^{\ell} - G_A^{\ell})(G_V^d - G_A^d) \right]}{16\sqrt{2}\pi\,\hat{G}_F\,N_{VA}^{\ell d}},$$

$$+ \frac{\left[\left(C_{\ell q}^{(1)} + C_{\ell q}^{(3)} \right) (G_V^{\ell} + G_A^{\ell})(G_V^d + G_A^d) \right]}{16\sqrt{2}\pi\,\hat{G}_F\,N_{VA}^{\ell d}} + \frac{\hat{\alpha}P(s)\left(\pm C_{\ell d} + C_{ed} + C_{\ell q}^{(1)} + C_{\ell q}^{(3)} \right)}{96s\hat{G}_F^2 N_{VA}^{\ell d}}.$$

$$N_{VA}^{\ell f} = (G_A^{\ell} G_V^{\ell} G_A^f G_V^f), \quad P(s) = \left(s/\hat{m}_Z^2 - 1 \right), \quad G_{VA}^i = \frac{(G_V^i)^2 + (G_A^i)^2}{(G_A^i G_V^i)^2}, \quad \delta G_{ijkl}^{\ell} = \frac{\delta g_i^{\ell}}{G_j^{\ell}} + \frac{\delta g_k^{\ell}}{G_l^{\ell}}.$$

$$\text{(B.5)}$$

The data from TRISTAN, PEP, PETRA and LEPII include total cross section measurements and forward backward asymmetries for various final state fermions. The data are given in Tables.2,3,6,7,8. The TRISTAN experiments were run at $\sqrt{s} \sim 60$ GeV, PEP and PETRA at $\sqrt{s} \sim 29$ GeV, and LEP II at energies $130 \leq \sqrt{s} \leq 209$ GeV. The angular dependence in Eqn.B.1, and the different $\sqrt{s}$ values projects out different operator combinations. The contributions to the total cross section (assuming total acceptance of the final state fermions in the detector) leads to

$$\delta\left(\sigma_{e^+e^- \to f\bar{f}} \right) = \frac{16}{3}\left(\frac{s\,F_1^{\ell f}}{P(s)} \right) \hat{G}_F^2\,N_c\,N_{VA}^{\ell f}, \tag{B.6}$$

Input parameters	Value	Ref.
$\hat{m}_Z$	91.1875 ± 0.0021	[32, 59, 60]
$\hat{G}_F$	$1.1663787(6) \times 10^{-5}$	[32, 60]
$\hat{\alpha}_{ew}$	$1/137.035999074(94)$	[32, 60]
$\hat{m}_h$	$125.09 \pm 0.21 \pm 0.11$	[61]
$\hat{m}_t$	$173.21 \pm 0.51 \pm 0.71$	[32]
$\hat{\alpha}_s$	0.1185	[32]
$\Delta\hat{\alpha}$	0.0590	[31]

Table 4. Input parameters values

Observable	Experimental Value	Ref.	SM Theoretical Value	Ref.
$\hat{m}_Z$[GeV]	91.1875 ± 0.0021	[59]	-	-
M_W[GeV]	80.385 ± 0.015	[62]	80.365 ± 0.004	[63]
σ_h^0 [nb]	41.540 ± 0.037	[59]	41.488 ± 0.006	[31]
Γ_Z[GeV]	2.4952 ± 0.0023	[59]	2.4943 ± 0.0005	[31]
R_ℓ^0	20.767 ± 0.025	[59]	20.752 ± 0.005	[31]
R_b^0	0.21629 ± 0.00066	[59]	0.21580 ± 0.00015	[31]
R_c^0	0.1721 ± 0.0030	[59]	0.17223 ± 0.00005	[31]
A_{FB}^ℓ	0.0171 ± 0.0010	[59]	0.01626 ± 0.00008	[64]
A_{FB}^c	0.0707 ± 0.0035	[59]	0.0738 ± 0.0002	[64]
A_{FB}^b	0.0992 ± 0.0016	[59]	0.1033 ± 0.0003	[64]

Table 5. Experimental and theoretical values of the LEPI observables used in constructing the χ^2 constraint functions. The results are grouped in terms of the precision of the measurements made. The entries above the double line are measured to better than percent accuracy, the entries below the double line are measured to an accuracy of a few percent.

while some contributions to the forward-backward asymmetries are proportional to

$$\delta\left(\sigma_{e^+e^- \to f\bar{f}}\right)_{F-B} = \left(\frac{s F_2^{\ell f}}{P(s)}\right) \hat{G}_F^2 N_c N_{VA}^{\ell f}. \tag{B.7}$$

For the detectors taking data at the TRISTAN accelerator (AMY,VENUS and TOPAZ) we approximate the angular acceptance by $-0.6 \leq \cos\theta \leq 0.6$ [17] giving the weighted contributions

$$\delta\left(\sigma_{e^+e^- \to f\bar{f}}\right)_{TRIS} \simeq 2.6 \left(\frac{s F_1^{\ell f}}{P(s)}\right) \hat{G}_F^2 N_c N_{VA}^{\ell f}, \tag{B.8}$$

$$\delta\left(\sigma_{e^+e^- \to f\bar{f}}\right)_{F-B}^{TRIS} \simeq 0.36 \left(\frac{s F_2^{\ell f}}{P(s)}\right) \hat{G}_F^2 N_c N_{VA}^{\ell f}. \tag{B.9}$$

---

[17]This approximation is based on direct examination of Ref. [65].

Observable	$\sqrt{s}$[GeV]	Experimental Value	Ref.	SM Theoretical Value	Ref.
σ_{had} [pb]	207	$17.316 \pm 0.212 \pm 0.083$	[51]	17.42 ± 0.0401	[52]
	205	$18.137 \pm 0.282 \pm 0.087$	[51]	17.85 ± 0.0411	[52]
	202	$18.873 \pm 0.408 \pm 0.098$	[51]	18.55 ± 0.0427	[52]
	200	$19.170 \pm 0.283 \pm 0.095$	[51]	19.03 ± 0.0438	[52]
	196	$20.307 \pm 0.294 \pm 0.096$	[51]	20.08 ± 0.0462	[52]
	192	$22.064 \pm 0.507 \pm 0.107$	[51]	21.22 ± 0.0488	[52]
	189	$22.492 \pm 0.206 \pm 0.119$	[51]	22.14 ± 0.0509	[52]
	183	$24.599 \pm 0.393 \pm 0.182$	[51]	24.21 ± 0.0557	[52]
	172	$29.350 \pm 0.989 \pm 0.336$	[51]	29.01 ± 0.0667	[52]
	161	$37.166 \pm 1.063 \pm 0.398$	[51]	35.53 ± 0.0817	[52]
	136	$66.984 \pm 1.954 \pm 0.630$	[51]	67.11 ± 0.154	[52]
	130	$82.445 \pm 2.197 \pm 0.766$	[51]	83.52 ± 0.192	[52]
	57.77	$143.6 \pm 1.5 \pm 4.5$	[58]	$142.2 \times (1 \pm 1\%)^\star$	[58]
$\sigma_{e^+e^- \to b\bar{b}}$ [pb]	58	$13.1 \pm 2.9 \pm 1.0$	[66]	$15 \times (1 \pm 1\%)^\star$	[66]
$\sigma_{e^+e^- \to c\bar{c}}$ [pb]	58	$55.9 \pm 8.8 \pm 7.9$	[66]	$41 \times (1 \pm 1\%)^\star$	[66]
$\frac{\sigma_{e^+e^- \to b\bar{b}}}{\sigma_{e^+e^- \to \text{Had}}}$	58	0.36 ± 0.05	[34]	$0.30 \times (1 \pm 1\%)^\star$	[34]
$\frac{\sigma_{e^+e^- \to c\bar{c}}}{\sigma_{e^+e^- \to \text{Had}}}$	58	0.13 ± 0.02	[34]	$0.13 \times (1 \pm 1\%)^\star$	[34]

Table 6. Experimental and theoretical values of pair production of coloured fermion pairs. See Section 2 for the fit methodology employed.

For PEP and PETRA, a reasonable approximation for the angular acceptance is $|\cos\theta| < 0.80$ which is an average of the one used for muon and tau final state pair production. The angular acceptance of the LEP experiments is superior but varies between the experiments. As a reasonable approximation we use the angular acceptance of $-0.9 \leq \cos\theta \leq 0.9$. This choice is informed by Ref. [51].

B.1.1 Forward-Backward Asymmetries for u, d, ℓ

Observable	$\sqrt{s}$[GeV]	Experimental Value	Ref.	SM Theoretical Value	Ref.
A^c_{FB}	58	-0.17 ± 0.14	[34]	$-0.48 \times (1 \pm 1\%)^\star$	[34]
A^b_{FB}	58	-0.20 ± 0.16	[34]	$-0.43 \times (1 \pm 1\%)^\star$	[34]

Table 7. Experimental and theoretical values of A_{FB}.

The shift in the FB Asymmetries off the Z pole are obtained from the general formula

$$\delta A_{FB}^{0,f} = \frac{\left(\left(\sigma_{e^+e^- \to f\bar{f}}\right)_{F-B}\right)_{SM}}{\left(\sigma_{e^+e^- \to f\bar{f}}\right)_{SM}} \left(\frac{\delta(\sigma_{e^+e^- \to f\bar{f}})_{F-B}}{\left(\left(\sigma_{e^+e^- \to f\bar{f}}\right)_{F-B}\right)_{SM}} - \frac{\delta\sigma_{e^+e^- \to f\bar{f}}}{\left(\sigma_{e^+e^- \to f\bar{f}}\right)_{SM}}\right).$$

Where we can calculate $\delta(\sigma_{e^+e^- \to f\bar{f}})_{F-B}$ and use our previous expression for $\delta\sigma_{e^+e^- \to f\bar{f}}$ to get the full expression of $\delta A_{FB}^{0,f}$. For FB asymmetries near the Z pole, the previous expression simplifies to

$$\delta A_{FB}^{0,f} = \frac{3}{4}\left(\delta A_\ell A_f + A_f \delta A_\ell\right), \tag{B.10}$$

with

$$\delta A_f = (A_f)_{SM}\left(1 - \frac{2r_f^2}{1 + r_f^2}\right)\delta r_f \tag{B.11}$$

$$\delta r_f = \frac{\delta g_V^f}{G_V^f} - \frac{\delta g_A^f}{G_A^f} \tag{B.12}$$

$$A_f = 2\frac{G_V^f G_A^f}{(G_V^f)^2 + (G_A^f)^2}. \tag{B.13}$$

B.2 Bhabba scattering, $e^+e^- \to e^+e^-$

The shift in the $e^+e^- \to e^+e^-$ differential cross section differs from the case of $e^+e^- \to \bar{f}f$. In the limit of a vectorial coupling, and neglecting the mass of the vector boson, the structure of the equations describing Bhabba scattering [68] is well known. In this limit, a $s \leftrightarrow t$ interchange symmetry that corresponds to the indistinguishability of the initial and final state particles is present. We structure our presentation of the shift in Bhabba scattering to reflect this limit finding

$$\begin{aligned}
\delta\left(\frac{d\sigma_{e^+e^- \to e^+e^-}}{d\cos(\theta)}\right) &= \frac{2\hat{G}_F^2}{\pi s}\left[\frac{u^2 F_3^+ + s^2 F_3^-}{P(t)^2} + \frac{u^2 F_3^- + t^2 F_3^+}{P(s)^2} + \frac{2u^2 F_3^+}{P(s)P(t)}\right], \\
&+ \frac{2\sqrt{2}\hat{G}_F\hat{\alpha}}{s}\left[\frac{u^2 F_7^+ + t^2 F_7^-}{sP(s)} + \frac{u^2 F_7^+ + s^2 F_7^-}{tP(t)} + \frac{u^2 F_7^+}{tP(s)} + \frac{u^2 F_7^+}{sP(t)}\right], \\
&+ \frac{2\hat{G}_F}{\pi s}\left[F_4 u^2\left(\frac{1}{P(s)} + \frac{1}{P(t)}\right) + F_5\left(\frac{t^2}{P(s)} + \frac{s^2}{P(t)}\right)\right], \\
&+ \frac{\hat{\alpha}}{2s}\left[2\left(\frac{u^2}{s} + \frac{u^2}{t}\right)C_{LL/RR} + \left(\frac{t^2}{s} + \frac{s^2}{t}\right)C_{LR}\right]. \tag{B.14}
\end{aligned}$$

Where we have introduced

$$G_{VA}^\ell = \frac{(G_V^\ell)^2 + (G_A^\ell)^2}{(G_V^\ell G_A^\ell)^2}, \qquad\qquad \delta G_{ijkl}^\ell = \frac{\delta g_i^\ell}{G_j^\ell} + \frac{\delta g_k^\ell}{G_l^\ell},$$

$$N_{VA}^\ell = G_V^\ell G_A^\ell,$$

Obs.	$\sqrt{s}$	Exp.	Ref.	SM Value	Ref.
A_{FB}^{μ}	207	$0.535 \pm 0.028 \pm 0.004$	[51]	0.552 ± 0.000197	[52]
	205	$0.556 \pm 0.034 \pm 0.004$	[51]	0.5540 ± 0.000201	[52]
	202	$0.547 \pm 0.045 \pm 0.005$	[51]	0.5571 ± 0.000206	[52]
	200	$0.519 \pm 0.031 \pm 0.005$	[51]	0.5593 ± 0.000211	[52]
	196	$0.592 \pm 0.030 \pm 0.005$	[51]	0.5639 ± 0.000222	[52]
	192	$0.551 \pm 0.051 \pm 0.007$	[51]	0.5687 ± 0.000232	[52]
	189	$0.571 \pm 0.020 \pm 0.005$	[51]	0.5726 ± 0.000240	[52]
	183	$0.564 \pm 0.034 \pm 0.008$	[51]	0.5811 ± 0.000259	[52]
	172	$0.673 \pm 0.077 \pm 0.012$	[51]	0.5976 ± 0.000301	[52]
	161	$0.542 \pm 0.069 \pm 0.012$	[51]	0.6192 ± 0.000355	[52]
	136	$0.707 \pm 0.061 \pm 0.011$	[51]	0.6862 ± 0.000551	[52]
	130	$0.694 \pm 0.059 \pm 0.012$	[51]	0.7069 ± 0.000638	[52]
	57.8	$-0.303 \pm 0.027 \pm 0.008$	[53]	$-0.336 \times (1 \pm 0.1\%)^{\star}$	[53]
	57.77	-0.256 ± 0.017	[54]	$-0.262 \times (1 \pm 0.1\%)^{\star}$	[54]
	35	$-0.099 \pm 0.015 \pm 0.005$	[55]	$-0.092 \times (1 \pm 0.1\%)^{\star}$	[55]
	29	-0.0587 ± 0.0097	[56]	$-0.059 \times (1 \pm 0.1\%)^{\star}$	[67]
A_{FB}^{τ}	207	$0.590 \pm 0.034 \pm 0.010$	[51]	0.552 ± 0.000226	[52]
	205	$0.618 \pm 0.040 \pm 0.008$	[51]	0.5539 ± 0.000231	[52]
	202	$0.535 \pm 0.058 \pm 0.009$	[51]	0.5570 ± 0.000238	[52]
	200	$0.539 \pm 0.041 \pm 0.007$	[51]	0.5592 ± 0.000243	[52]
	196	$0.464 \pm 0.044 \pm 0.008$	[51]	0.5637 ± 0.000256	[52]
	192	$0.590 \pm 0.067 \pm 0.008$	[51]	0.5686 ± 0.000267	[52]
	189	$0.590 \pm 0.026 \pm 0.007$	[51]	0.5725 ± 0.000277	[52]
	183	$0.604 \pm 0.044 \pm 0.011$	[51]	0.5809 ± 0.000298	[52]
	172	$0.357 \pm 0.098 \pm 0.013$	[51]	0.5974 ± 0.000346	[52]
	161	$0.764 \pm 0.061 \pm 0.013$	[51]	0.6190 ± 0.000409	[52]
	136	$0.761 \pm 0.089 \pm 0.013$	[51]	0.6859 ± 0.000634	[52]
	130	$0.682 \pm 0.079 \pm 0.016$	[51]	0.7066 ± 0.000734	[52]
	57.8	$-0.291 \pm 0.040 \pm 0.019$	[53]	$-0.336 \times (1 \pm 0.1\%)^{\star}$	[53]
	57.77	$-0.2106 \pm 0.0167 \pm 0.0098$	[58]	$-0.262 \times (1 \pm 0.1\%)^{\star}$	[54]
	35	$-0.081 \pm 0.02 \pm 0.006$	[55]	$-0.092 \times (1 \pm 0.1\%)^{\star}$	[55]
	29	$-0.061 \pm 0.023 \pm 0.005$	[67]	$-0.059 \times (1 \pm 0.1\%)^{\star}$	[67]

Table 8. Experimental and theoretical values for various A_{FB} measurements.

$$F_3^{\pm} = 4(N_{VA}^{\ell})^3 G_{VA}^{\ell} \delta G_{VAAV}^{\ell} \pm 8(N_{VA}^{\ell})^2 \delta G_{VVAA}^{\ell}, \quad F_4 = \frac{1}{\sqrt{2}}(G_{AV}^{\ell\pm})^2 C_{LL/RR},$$

$$F_5 = -\frac{1}{2\sqrt{2}} G_{AV}^{\ell+} G_{AV}^{\ell-} C_{LR}, \qquad F_6^{\pm} = \pm 8(N_{VA}^{\ell})^2 - 2(G_{VA}^{\ell})^2(N_{VA}^{\ell})^4,$$

$$F_7^{\pm} = 2 G_V^{\ell} \delta g_V^{\ell} \pm 2 G_A^{\ell} \delta g_A^{\ell}, \qquad F_8^{\pm} = \left((G_V^{\ell})^2 \pm (G_A^{\ell})^2\right).$$

cosθ bin	$\sqrt{s}$	Exp. Value	Ref.	SM Value	Ref.
$[-0.90, -0.72]$	207	1.440 ± 0.196	[51]	$1.339 \times (1 \pm 0.2\%)^\star$	[51, 69]
$[0.27, 0.36]$	207	11.221 ± 0.615	[51]	$11.019 \times (1 \pm 0.2\%)^\star$	[51, 69]
$[0.81, 0.90]$	207	573.637 ± 6.024	[51]	$576.688 \times (1 \pm 0.2\%)^\star$	[51, 69]
$[-0.90, -0.72]$	205	1.102 ± 0.205	[51]	$1.355 \times (1 \pm 0.2\%)^\star$	[51, 69]
$[0.27, 0.36]$	205	10.607 ± 0.764	[51]	$11.200 \times (1 \pm 0.2\%)^\star$	[51, 69]
$[0.81, 0.90]$	205	587.999 ± 7.527	[51]	$586.205 \times (1 \pm 0.2\%)^\star$	[51, 69]
$[-0.90, -0.72]$	202	1.568 ± 0.368	[51]	$1.401 \times (1 \pm 0.2\%)^\star$	[51, 69]
$[0.27, 0.36]$	202	11.032 ± 1.113	[51]	$11.554 \times (1 \pm 0.2\%)^\star$	[51, 69]
$[0.81, 0.90]$	202	599.860 ± 10.339	[51]	$605.070 \times (1 \pm 0.2\%)^\star$	[51, 69]
$[-0.90, -0.72]$	200	1.483 ± 0.245	[51]	$1.420 \times (1 \pm 0.2\%)^\star$	[51, 69]
$[0.27, 0.36]$	200	9.506 ± 0.736	[51]	$11.773 \times (1 \pm 0.2\%)^\star$	[51, 69]
$[0.81, 0.90]$	200	604.986 ± 7.608	[51]	$617.718 \times (1 \pm 0.2\%)^\star$	[51, 69]
$[-0.90, -0.72]$	196	1.470 ± 0.261	[51]	$1.483 \times (1 \pm 0.2\%)^\star$	[51, 69]
$[0.27, 0.36]$	196	13.444 ± 0.856	[51]	$12.326 \times (1 \pm 0.2\%)^\star$	[51, 69]
$[0.81, 0.90]$	196	637.846 ± 8.003	[51]	$642.688 \times (1 \pm 0.2\%)^\star$	[51, 69]
$[-0.90, -0.72]$	192	1.300 ± 0.364	[51]	$1.539 \times (1 \pm 0.2\%)^\star$	[51, 69]
$[0.27, 0.36]$	192	12.941 ± 1.414	[51]	$12.800 \times (1 \pm 0.2\%)^\star$	[51, 69]
$[0.81, 0.90]$	192	655.724 ± 12.588	[51]	$669.173 \times (1 \pm 0.2\%)^\star$	[51, 69]
$[-0.90, -0.72]$	189	1.401 ± 0.161	[51]	$1.590 \times (1 \pm 0.2\%)^\star$	[51, 69]
$[0.27, 0.36]$	189	12.781 ± 0.576	[51]	$13.345 \times (1 \pm 0.2\%)^\star$	[51, 69]
$[0.81, 0.90]$	189	679.146 ± 5.773	[51]	$689.9893 \times (1 \pm 0.2\%)^\star$	[51, 69]

Table 9. Experimental and theoretical values of the LEPII observables $\sigma_{e^+e^- \to e^+e^-}$. For a theory error we take 0.2% for the legacy LEPII data, following the discussion in Ref. [70].

We use the LEPII data given in Table.9 for Bhabba scattering, which is a subset of LEP data. We have examined the bin dependence of the shifts in the SMEFT and chosen the bins in Table.9 to optimise sensitivity to possible shifts, while not oversampling Bhabba scattering data. This choice is driven by the fact that the Bhabba scattering data does not supply a correlation matrix.

C   Low energy precision measurements

Due to the large number of operators contributing in a general analysis of LEP data, and related $2 \to 2$ scattering data at lower energy colliders, it is of interest to extract constraints from yet other measurements. A useful source of information is to also incorporate bounds from neutrino Deep Inelastic Scattering (DIS) experiments.

We utilize bounds from neutrino-electron (CHARM and CHARM II [71, 72], and CALO [73]) and neutrino-nucleon scattering (at CDHS [74], CHARM [71], CCFR [75], and NuTeV

Obs.	$\sqrt{s}$[GeV]	Experimental Value	Ref.	SM Theoretical Value	Ref.
$g_V^{\nu_\mu e}$	$\sim 3-24$	-0.06 ± 0.07	[79]	$-0.0396 \pm 0.0002^\star$	[80]
$g_A^{\nu_\mu e}$	$\sim 3-24$	-0.54 ± 0.07	[79]	$-0.5064 \pm 0.0002^\star$	[80]
$g_V^{\nu_\mu e}$	$\sim 3-24$	-0.035 ± 0.017	[72]	$-0.0396 \pm 0.0002^\star$	[80]
$g_A^{\nu_\mu e}$	$\sim 3-24$	-0.503 ± 0.017	[72]	$-0.5064 \pm 0.0002^\star$	[80]
$g_V^{\nu_\mu e}$	~ 1	-0.107 ± 0.045	[73]	$-0.0396 \pm 0.0002^\star$	[80]
$g_A^{\nu_\mu e}$	~ 1	-0.514 ± 0.036	[73]	$-0.5064 \pm 0.0002^\star$	[80]

Table 10. Experimental and theoretical values of $g_V^{\nu e}$ and $g_A^{\nu e}$. The theoretical prediction and error is taken from Ref. [80] and is estimated by the leading Q dependent neglected correction, which is quoted as two orders of magnitude below ± 0.02.

[35]) experiments. From inelastic electron scattering (at SLAC E158 [76]) we incorporate bounds from low energy parity violating asymmetry measurements. Using data from polarized electron scattering experiments at SLAC (eDIS [77]) and the SAMPLE experiment [78] we extract bounds from Atomic Parity Violation measurements.

C.1 ν lepton scattering

For $\nu\, e^\pm \to \nu\, e^\pm$ scattering we calculate the shift of $\bar{g}_{V,A}^{\nu e}$, where these parameters are defined by the following Effective Lagrangian

$$\mathcal{L}_{\nu e} = -\frac{\hat{G}_F}{\sqrt{2}} \left[\bar{e}\gamma^\mu \left((\bar{g}_V^{\nu e}) - (\bar{g}_A^{\nu e})\gamma^5 \right) e \right] \left[\bar{\nu}\gamma_\mu \left(1 - \gamma^5 \right) \nu \right]. \tag{C.1}$$

Recalling that $\delta g_V^\nu = \delta g_A^\nu$, $g_V^x = \frac{T_3}{2} - Q_x s_{\hat\theta}^2$, $g_A^x = \frac{T_3}{2}$ and $g_{V,A}^{\ell,W} = \frac{1}{2}$, the shifts are then $\bar{g}_V^{\nu e} = g_V^{\nu e} + \delta g_V^{\nu e}$, $\bar{g}_A^{\nu e} = g_A^{\nu e} + \delta g_A^{\nu e}$ where

$$\delta(g_V^{\nu e}) = 2 \left(\delta g_V^\ell - 2\delta g_V^{\ell,W_\pm} \right) + 4\delta g_V^\nu \left(-\frac{1}{2} + 2s_{\hat\theta}^2 \right) - \frac{1}{2\sqrt{2}\hat{G}_F} \left(2C_{\ell\ell} + C_{\ell e} \right) - \frac{\delta M_W^2}{M_W^2}, \tag{C.2}$$

$$\delta(g_A^{\nu e}) = 2 \left(\delta g_A^\ell - 2\delta g_A^{\ell,W_\pm} \right) - 2\delta g_V^\nu - \frac{1}{2\sqrt{2}\hat{G}_F} \left(2C_{\ell\ell} - C_{\ell e} \right) - \frac{\delta M_W^2}{M_W^2}. \tag{C.3}$$

these shifts add the contributions of W and Z exchange. Depending on the neutrino flavour some terms are absent. The shift that is relevant for $g_{A,V}^{\nu_\mu e}$ does not have a δM_W^2 or $\delta g_{V,A}^{\ell,W_\pm}$ contribution, whereas a shift for $g_{A,V}^{\nu_\mu \mu}$ has both contributions. We use the later for neutrino trident production. We use the former for fitting to the data in Table. 10 to constrain these shifts.

C.2 ν Nucleon scattering

For $\nu N \to \nu X$ scattering, we consider a Z exchange in the SMEFT. We define two parameters $\bar{\epsilon}_L^q$ and $\bar{\epsilon}_R^q$ for q=u,d by the following Effective Lagrangian

$$\mathcal{L}_{\nu q}^{NC} = -\frac{\hat{G}_F}{\sqrt{2}} \left[\bar{\nu}\gamma^\mu \left(1 - \gamma^5\right)\nu \right] \left[\bar{\epsilon}_L^q \bar{q}\gamma_\mu \left(1 - \gamma^5\right)q + \bar{\epsilon}_R^q \bar{q}\gamma_\mu \left(1 + \gamma^5\right)q \right]. \tag{C.4}$$

At tree level in the SM we have $(\epsilon_L^q)_{SM} = G_V^q + G_A^q$ and $(\epsilon_R^q)_{SM} = G_V^q - G_A^q$ where $G_{V/A}^q$ are the Z couplings of the quark. The redefinition of the Z couplings and the corrections due to ψ^4 operators lead to a shift in ϵ_L^q and ϵ_R^q of the form $\bar{\epsilon}_{L/R}^q = \epsilon_{L/R}^q + \delta\epsilon_{L/R}^q$ with $\delta\epsilon_{L/R}^q$ given for up and down quarks

$$\delta\epsilon_L^u = -\frac{1}{2\sqrt{2}\hat{G}_F} \left(C_{\ell q}^{(1)} + C_{\ell q}^{(3)} \right) + \delta g_V^u + \delta g_A^u + 4\delta g_V^\nu (\epsilon_L^u)_{SM}, \tag{C.5}$$

$$\delta\epsilon_L^d = -\frac{1}{2\sqrt{2}\hat{G}_F} \left(C_{\ell q}^{(1)} - C_{\ell q}^{(3)} \right) + \delta g_V^d + \delta g_A^d + 4\delta g_V^\nu (\epsilon_L^d)_{SM}, \tag{C.6}$$

$$\delta\epsilon_R^u = -\frac{1}{2\sqrt{2}\hat{G}_F} C_{\ell u} + \delta g_V^u - \delta g_A^u + 4\delta g_V^\nu (\epsilon_R^u)_{SM}, \tag{C.7}$$

$$\delta\epsilon_R^d = -\frac{1}{2\sqrt{2}\hat{G}_F} C_{\ell d} + \delta g_V^d - \delta g_A^d + 4\delta g_V^\nu (\epsilon_R^d)_{SM}. \tag{C.8}$$

Here we used $\delta g_V^\nu = \delta g_A^\nu$ and $G_V^\nu = G_A^\nu = \frac{1}{4}$. In terms of some common notation used in Ref. [32, 80] $\epsilon_L^f = g_{LL}^f$, $\epsilon_R^f = g_{LR}^f$. For $\nu N \to \ell X$ and the inverse process, W exchange defines $\bar{\Sigma}_L^{ij}$ by the following Lagrangian

$$\mathcal{L} = -\frac{\hat{G}_F}{\sqrt{2}} \left[\bar{\ell}\gamma^\mu \left(1 - \gamma^5\right)\nu \right] \left[\bar{\Sigma}_L^{ij} \bar{u}_i\gamma_\mu \left(1 - \gamma^5\right)d_j \right] + h.c, \tag{C.9}$$

where for the tree level SM result $(\Sigma_L^{ij})_{SM} = V_{CKM}^{ij}$, where V_{CKM} is the Cabibbo-Kobyashi-Maskawa matrix. $(\Sigma_L^{ij})_{SM}$ receives corrections from W couplings redefinitions and the M_W redefinition, so that $\bar{\Sigma}_L^{ij} = (\Sigma_L^{ij})_{SM} + \delta\Sigma_L^{ij}$ with

$$\delta\Sigma_L^{ij} = \frac{\delta M_W^2}{M_W^2} V_{CKM}^{ij} + 2\,\delta g_V^{q,W} V_{CKM}^{ij} + 2\,\delta g_V^{\ell,W} V_{CKM}^{ij} - \frac{1}{\sqrt{2}\hat{G}_F} C_{\ell q}^{(3)} V_{CKM}^{ij}. \tag{C.10}$$

Where we used that $\delta g_V^{x,W} = \delta g_A^{x,W}$. In principle one can include in the Lagrangian a term of the form $\bar{\Sigma}_R^{ij}$, with a right handed projector. This term is zero in the SM, but can be generated by the operator $Q_{\ell edq}$ in the SMEFT. These corrections are proportional to Yukawa terms and so vanish when we consider massless fermions, and are neglected.

Analyses of ν Nucleon scattering rely on relations between charged and neutral current process parameterizing effective left and right handed couplings on Isoscalar targets [81]

$$\frac{d^2\,\sigma(\nu N \to \nu X)}{dx\,dy} = g_{L,eff}^2 \frac{d^2\,\sigma(\nu N \to \mu^- X)}{dx\,dy} + g_{R,eff}^2 \frac{d^2\,\sigma(\bar{\nu} N \to \mu^+ X)}{dx\,dy}. \tag{C.11}$$

for the scattering variables

$$x = \frac{-q^2}{2\,p_N \cdot q}, \qquad y = \frac{p_N \cdot q}{p_N \cdot p_\nu}, \tag{C.12}$$

defined in terms of the momentum transfer q^2, the nucleon momentum p_N and the neutrino momentum p_ν. These effective couplings receive corrections in the SMEFT so that $\bar{g}^2_{L/R,eff} = g^2_{L/R,eff} + \delta g^2_{L/R,eff}$ and

$$\bar{g}^2_{L/R,eff} = \sum_{i,j} \left[\left| \bar{\epsilon}^{u^i}_{L/R} \right|^2 + \left| \bar{\epsilon}^{d^j}_{L/R} \right|^2 \right] \left| (\bar{\Sigma}^{ij}_L) \right|^{-2}, \tag{C.13}$$

$$\bar{h}^2_{L/R,eff} = \sum_{i,j} \left[\left| \bar{\epsilon}^{u^i}_{L/R} \right|^2 - \left| \bar{\epsilon}^{d^j}_{L/R} \right|^2 \right] \left| (\bar{\Sigma}^{ij}_L) \right|^{-2}. \tag{C.14}$$

Although these expressions are general for all flavours, we will implicitly restrict our attention to the case of only first generation quarks in the target nucleon when considering PDFs. Data on ν Nucleon scattering tends to be reported as a ratio of cross sections

$$R^\nu = \frac{\sigma\,(\nu N \to \nu X)}{\sigma\,(\nu N \to \ell^- X)} = g^2_{L,eff} + r g^2_{R,eff}, \quad R^{\bar{\nu}} = \frac{\sigma\,(\bar{\nu} N \to \bar{\nu} X)}{\sigma\,(\bar{\nu} N \to \ell^+ X)} = g^2_{L,eff} + \frac{g^2_{R,eff}}{r}(\text{C.15})$$

The factor r in an ideal experiment with full acceptance (in the absence of sea quarks) is given by $r = 1/3$. When fitting shifts to the SM expectation we use a supplied value of r if it is simultaneously fit to, as in the case of CHARM [71]. Otherwise we use $r \sim 0.44$. In principle further corrections in the SMEFT can be present in r. Here we have assumed that the effect of the SMEFT on the parton and anti-parton distributions of the neutrons and protons is negligible compared to the corrections that we include in Eqn. C.4,C.10. This choice is motivated out of our adoption of a $\mathrm{U}(3)^5$ scenario, and the neglect of the flavour violating effects of $\mathcal{L}_4$ feeding into $\mathcal{L}_6$. These assumptions, and the implicit assumption that these corrections scale as $\Lambda^2_{QCD}/\Lambda^2$, motivate neglecting these effects. This introduces a further theoretical error of the form

$$\Delta_{R^\nu} \sim \frac{\Lambda^2_{QCD}}{\bar{v}^2_T} \frac{\bar{v}^2_T}{\Lambda^2} \sim 2 \times 10^{-5} \frac{\bar{v}^2_T}{\Lambda^2}. \tag{C.16}$$

This error is neglected in the fit. CCFR reports data in terms of the parameter κ which is given by

$$\kappa = 1.7897\,g^2_{L,eff} + 1.1479 g^2_{R,eff} - 0.0916\,h^2_{L,eff} - 0.0782\,h^2_{R,eff} \tag{C.17}$$

We use the data given in Table 11 to fit, expanding the effective couplings to linear order in the SMEFT shifts.

Observable	$Q\,[\text{GeV}]$	Experimental Value	r	Ref.	SM Value	Ref.
R^ν	$\gtrsim 4$	0.3093 ± 0.0031	0.456	[71]	$0.3178 \times (1 \pm 2\%)^\star$	[32, 80]
$R^{\bar\nu}$	$\gtrsim 4$	0.390 ± 0.014	0.456	[71]	$0.3691 \times (1 \pm 2\%)^\star$	[32, 80]
κ	$\gtrsim 4$	0.5820 ± 0.0041	-	[75]	$0.5832 \times (1 \pm 0.2\%)^\star$	[32, 80]
$g^2_{L,eff}$	~ 20	0.30005 ± 0.00137	-	[35]	0.3043 ± 0.002	[32, 80]
$g^2_{R,eff}$	~ 20	0.03076 ± 0.00110	-	[35]	0.0295 ± 0.002	[32, 80]

Table 11. Experimental and theoretical values of R^ν and $R^{\bar\nu}$. Theory predictions are obtained by using the leading order Llewellyn-Smith relations with a fitted r in the case of CHARM, with input parameters for the SM $g_{L,R}$ as quoted in the PDG [32]. Similarly the relation reported in Eqn.C.17 is used with input values for $g_{L,R}$, $h_{L,R}$ taken from the PDG for κ. The NuTeV results are also compared to the quoted $g_{L,R}$ values from the PDG. The theoretical predictions for ν Nucleon scattering are subject to theoretical uncertainties due to higher order neglected corrections in perturbation theory (beyond one loop order generally) and harder to quantify PDF and nuclear form factor uncertainties. As the determined value of r feeds into the theoretical prediction for CHARM which has errors of a few percent we take this as the dominant theoretical error. The CCFR collaboration quoted a SM prediction [75] with 0.2% theoretical error. We use this value in the modified theory prediction used. The interpretation of the NuTeV result is potentially subject to large uncertainties as detailed in the PDG [32]. We assign the neglected isospin violating PDF correction (detailed in Ref. [82], Eqn.(34)) as a theory error.

C.2.1 Neutrino Trident Production

Neutrino trident production is the pair production of leptons from the scattering of a neutrino off the Coulomb field of a nucleus, $\nu\,N \to \nu\,N\,\ell^+\,\ell^-$. The scattering of such highly relativistic neutrinos is well approximated by the Equivalent Photon Approximation (EPA) [83, 84] and has been recently discussed in the context of Z' models in Refs.[85, 86]. The SM calculation of this process is well known, see Refs.[87, 88]. Here we follow the discussion and notation in Ref. [86, 87]. The effective Lagrangian for this interaction is given by Eqn.C.1. The constraint on the SMEFT is through the ratio of the partonic cross sections

$$\frac{\bar\sigma_{SMEFT}}{\sigma_{SM}} = \frac{(\bar g_V^{\nu_e e})^2 + (\bar g_A^{\nu_e e})^2}{(g_V^{\nu_e e})^2_{SM} + (g_A^{\nu_e e})^2_{SM}}. \tag{C.18}$$

As the effects we consider are heavier than the SM W, Z bosons, we assume that the subsequent phase space integrals over the partonic process are not modified. Due to this assumption we can directly constrain this ratio with the entries in Table. 12. Note that at tree level in the SM $(g_V^{\nu_e e})_{SM} = \frac{1}{2} + 2\,s_{\hat\theta}^2$ and $(g_A^{\nu_e e})_{SM} = \frac{1}{2}$. We expand out to linear order in the shifts $\delta g_V^{\nu_e e}, \delta g_A^{\nu_e e}$ when constraining this ratio.

Observable	$E_\nu[\text{GeV}]$	Experimental Value	Ref.	SM Theoretical Value	Ref.
$\frac{\sigma_{CHARMII}}{\sigma_{SM}}$	~ 30	1.58 ± 0.57	[89]	1	[86, 87]
$\frac{\sigma_{CCFR}}{\sigma_{SM}}$	~ 160	0.82 ± 0.28	[90]	1	[86, 87]

Table 12. Experimental and theoretical values of Neutrino trident production, as a ratio to the SM cross section. Due to the variation in the reported NuTeV results, depending on the background treatment, we do not include the NuTeV result in the fit. The effective energy transfer in Neutrino trident production is a fraction of the Neutrino beam energy quoted, so that using an effective lagrangian is justified. Theoretical errors have been absorbed into the error on the quoted ratio in this case, and we assume that the extra SMEFT error is subdominant to the $\sim 35\%$ error in the reported ratios.

C.3 Atomic Parity Violation

For Atomic Parity Violation (APV) the standard Effective Lagrangian is given by

$$\mathcal{L}_{eq} = \frac{\hat{G}_F}{\sqrt{2}} \left[\sum_q \bar{g}_{AV}^{eq} \left(\bar{e}\gamma_\mu\gamma^5 e \right) \left(\bar{q}\gamma^\mu q \right) + \bar{g}_{VA}^{eq} \left(\bar{e}\gamma_\mu e \right) \left(\bar{q}\gamma^\mu\gamma^5 q \right) \right], \tag{C.19}$$

Where in the SM we have $(g_{AV}^{eq})_{SM} = 8\, G_V^q\, G_A^\ell$ and $(g_{VA}^{eq})_{SM} = 8\, G_A^q\, G_V^\ell$. We are interested in the corrections that g_{AV}^{eq} and g_{VA}^{eq} get when $q = u, d$. The effective shifts are

$$\delta g_{AV}^{eu} = \frac{1}{2\sqrt{2}\hat{G}_F} \left(-C_{\ell q}^{(1)} + C_{\ell q}^{(3)} - C_{\ell u} + C_{eu} + C_{qe} \right) + 2\left(1 - \frac{8}{3}s_{\hat{\theta}}^2\right)\delta g_A^\ell$$
$$- 2\delta g_V^u, \tag{C.20}$$

$$\delta g_{VA}^{eu} = \frac{1}{2\sqrt{2}\hat{G}_F} \left(-C_{\ell q}^{(1)} + C_{\ell q}^{(3)} + C_{\ell u} + C_{eu} - C_{qe} \right) + 2\delta g_A^u \left(-1 + 4s_{\hat{\theta}}^2\right)$$
$$+ 2\delta g_V^\ell, \tag{C.21}$$

$$\delta g_{AV}^{ed} = \frac{1}{2\sqrt{2}\hat{G}_F} \left(-C_{\ell q}^{(1)} - C_{\ell q}^{(3)} - C_{\ell d} + C_{ed} + C_{qe} \right) + 2\left(-1 + \frac{4}{3}s_{\hat{\theta}}^2\right)\delta g_A^\ell$$
$$- 2\delta g_V^d, \tag{C.22}$$

$$\delta g_{VA}^{ed} = \frac{1}{2\sqrt{2}\hat{G}_F} \left(-C_{\ell q}^{(1)} - C_{\ell q}^{(3)} + C_{\ell d} + C_{ed} - C_{qe} \right) + 2\delta g_A^d \left(-1 + 4s_{\hat{\theta}}^2\right)$$
$$- 2\delta g_V^\ell. \tag{C.23}$$

From these four couplings we define a set of four others couplings $\bar{g}_{AV/VA}^{ep} = 2\bar{g}_{AV/VA}^{eu} + \bar{g}_{AV/VA}^{ed}$ and $\bar{g}_{AV}^{en} = \bar{g}_{AV/VA}^{eu} + 2\bar{g}_{AV/VA}^{ed}$. These new couplings are shifted from their SM values by

$$\delta g_{AV/VA}^{ep} = 2\delta g_{AV/VA}^{eu} + \delta g_{AV/VA}^{ed}, \tag{C.24}$$

$$\delta g_{AV/VA}^{en} = \delta g_{AV/VA}^{eu} + 2\delta g_{AV/VA}^{ed}. \tag{C.25}$$

We then define the weak charge $Q_W^{Z,N}$ of an element X_Z^A by [32, 80, 91]

$$Q_W^{Z,N} = -2\left[Z\left(g_{AV}^{ep} + 0.00005\right) + N\left(g_{AV}^{en} + 0.00006\right)\right]\left(1 - \frac{\bar{\alpha}}{2\pi}\right), \tag{C.26}$$

Observable	$\sqrt{s}$[GeV]	Experimental Value	Ref.	SM Theoretical Value	Ref.
$Q_W^{81,124}(Tl)$	$\lesssim 1$	-114.2 ± 3.8	[92]	-116.9 ± 3.5	[32]
$Q_W^{55,78}(Cs)$	$\lesssim 1$	-71.0 ± 1.8	[93]	$-72.65 \pm 0.28 \pm 0.34$	[94]

Table 13. Experimental and theoretical values of the weak charges.

so that the shift in $Q_W^{Z,N}$ is

$$\delta Q_W^{Z,N} = -2 \left[Z \delta g_{AV}^{ep} + N \delta g_{AV}^{en} \right] \left(1 - \frac{\hat{\alpha}}{2\pi} \right). \tag{C.27}$$

We use the precise determinations of $Q_W^{Z,N}$ for Thallium(Tl) and Cesium (Cs) given in Table 13 to construct constraints from these measurements.

C.4 Parity Violating Asymmetry in eDIS

For inelastic polarized electron scattering $e_{L,R} N \to e X$ the right-left asymmetry A is defined as [32]:

$$A = \frac{\sigma_R - \sigma_L}{\sigma_R + \sigma_L}, \tag{C.28}$$

where

$$\frac{A}{Q^2} = a_1 + a_2 \frac{1 - (1-y)^2}{1 + (1-y)^2} \text{ with :} \tag{C.29}$$

$$a_1 = \frac{3\hat{G}_F}{5\sqrt{2}\pi\hat{\alpha}} \left(g_{AV}^{eu} - \frac{1}{2} g_{AV}^{ed} \right), \tag{C.30}$$

$$a_2 = \frac{3\hat{G}_F}{5\sqrt{2}\pi\hat{\alpha}} \left(g_{VA}^{eu} - \frac{1}{2} g_{VA}^{ed} \right). \tag{C.31}$$

Moving to the SMEFT, $g_{AV/VA}^{eq}$ get corrected so that: $\bar{g}_{AV/VA}^{eq} = g_{AV/VA}^{eq} + \delta g_{AV/VA}^{eq}$ so that a_1 and a_2 receive the corrections

$$\delta a_1 = \frac{3\hat{G}_F}{5\sqrt{2}\pi\hat{\alpha}} \left(\delta g_{AV}^{eu} - \frac{1}{2} \delta g_{AV}^{ed} \right), \tag{C.32}$$

$$\delta a_2 = \frac{3\hat{G}_F}{5\sqrt{2}\pi\hat{\alpha}} \left(\delta g_{VA}^{eu} - \frac{1}{2} \delta g_{VA}^{ed} \right). \tag{C.33}$$

We use the data in Table 14 to bound deviations in eDIS experiments. These results are again subject to theoretical uncertaintes in the form of isospin violating effects, nuclear form factors, etc. For example, measurements of inelastic electron scattering are also sensitive to the magnetic strange quark form factor. The SAMPLE experiments [78, 95] measured the parity-violating asymmetry A for different momentum transfer Q^2 and different targets. SAMPLE

Observable	$\sqrt{s}$[GeV]	Experimental Value	Ref.	SM Value	Ref.
a_1	~ 1	$(-9.7 \pm 2.6).10^{-5}$	[77]	$-7.7 \times 10^{-5} \times (1 \pm 0.2\%)^{\star}$	[32]
a_2	~ 1	$(4.9 \pm 8.1).10^{-5}$	[77]	$-1.0 \times 10^{-5} \times (1 \pm 0.2\%)^{\star}$	[32]
$A_D(Q^2 = 0.038)$	0.12	$-3.51 \pm 0.57 \pm 0.58$	[95]	-2.79 ± 0.21	[95]
$A_D(Q^2 = 0.091)$	0.22	$-7.77 \pm 0.73 \pm 0.62$	[95]	-8.33 ± 0.43	[95]

Table 14. Experimental and theoretical values of a_1 and a_2. The theory error for a_1, a_2 is obtained from the leading PDF isospin correction estimate of Ref. [82] and the theory value is constructed using the quoted values of the PDG for the effective couplings. For A_D we use the SM value quoted in the experimental result, which is given in ppm units.

I were performed on a Hydrogen target, while SAMPLE II was performed on a deuterium target, both at $Q^2 = 0.1$. The first two SAMPLE measurements allow an extraction of the magnetic strange quark form factor which is then used in SAMPLE III, carried out on deuterium targets, but at $Q^2 = 0.038(\text{GeV/c})^2$. The results from the HAPPEx experiments [96] are not used as the SM is assumed in their analysis [80]. Similar comments apply to the results of the PVA4 measurements at the MAMI microton.

C.5 Møller scattering

For the Parity Violation Asymmetry (A_{PV}) in Møller scattering, we use the standard Effective Lagrangian

$$\mathcal{L}_{ee} = \hat{G}_F \sqrt{2} g_{AV}^{ee} \left(\bar{e} \gamma^{\mu} \gamma^5 e \right) \left(\bar{e} \gamma_{\mu} e \right). \tag{C.34}$$

The constraints on A_{PV} are determined by examining fixed target polarized Møller scattering data ($e^- e^- \to e^- e^-$). In the SM we have $g_{AV}^{ee} = 8 G_V^{\ell} G_A^{\ell} = \frac{1}{2} \left(1 - 4 s_{\hat{\theta}}^2 \right)$. In the SMEFT we have the correction

$$\delta g_{AV}^{ee} = \frac{1}{2\sqrt{2}\hat{G}_F} \left(-C_{\ell\ell} + C_{ee} \right) - 2\delta g_V^{\ell} - 2 \left(1 - 4 s_{\hat{\theta}}^2 \right) \delta g_A^{\ell}, \tag{C.35}$$

The parity violating asymmetry A_{PV} is then expressed as

$$\frac{A_{PV}}{Q^2} = -2 g_{AV}^{ee} \frac{\hat{G}_F}{\sqrt{2}\pi\hat{\alpha}} \frac{1-y}{1 + y^4 + (1-y)^4}. \tag{C.36}$$

Here $Q^2 \geq 0$ is the momentum transfer and y is the fractional energy transfer in the scattering $y \simeq Q^2/s$. The SLAC E158 experiment [76] measured Møller scattering at $Q^2 = 0.026\text{GeV}^2$ reporting $A_{PV} = (-131 \pm 14 \pm 10) \times 10^{-9}$.[18]

---

[18]The 2014 EW PDG review quotes a normalization of the Effective Lagrangian in Eqn.C.34 that differs from Eqn.C.34 result by a factor of 2. The value quoted in Table 10.3 of the EW review substituted into Eq. 10.27 of the EW review gives the correct SM result, which agrees with Ref. [97], as we have verified. We find the normalization of g_{AV}^{ee} in Table 10.3 corresponds to the normalization in Eqn. C.34, and have corrected for this in our numerical update. We thank Jens Erler for communication regarding this point.

Obs.	$\sqrt{s}$[GeV]	Experimental Value	Ref.	SM Theoretical Value	Ref.
A_{PV}	0.2GeV	$(-131 \pm 14 \pm 10) \times 10^{-9}$	[76]	$(-126 \pm 2) \times 10^{-9}$	[76]

Table 15. Experimental and theoretical values of Parity Violation Asymmetry.

D   Universality in β decays

As discussed in Ref.[50] in a model independent context,[19] it is possible to place bounds on combinations of four fermion operators and $W^\pm$ vertex corrections by comparing the extraction of G_F from $\mu^- \to e^- + \bar{\nu}_e + \nu_\mu$ decays to its determined value in other semileptonic β decays. This constraint is presented in terms of a bound on the unitarity of the CKM matrix, assuming $U(3)^5$ universality in the SMEFT. We use the bound determined in Ref.[99] for this purpose, which quotes

$$|V_{CKM}|^2 = |V_{ud}^{meas}|^2 + |V_{us}^{meas}|^2 + |V_{ub}^{meas}|^2, \tag{D.1}$$

$$= 1 + (-0.1 \pm 0.6) \times 10^{-3}, \tag{D.2}$$

after a careful examination of the (SM) theoretical and experimental errors present in the determination of the CKM matrix elements phenomenologically. Formally, the fit performed in Ref.[99] should be redone with the inclusion of a SMEFT error for each observable following the discussion in Section 2.4.1. This is beyond the scope of this work, and as an approximation we add a numerical Δ_{SMEFT} error in quadrature with the quoted error above that is consistent with the theory error assigned to other observables, when performing the joint fit. This means that we treat this constraint, which is the result of a global fit of many observables, as a single net observable for constraints in the SMEFT. In the Warsaw basis, this constraint is a bound on the following combination of operators

$$\delta|V_{CKM}|^2 = \frac{\sqrt{2}}{\hat{G}_F} \left(-C_{\ell q}^{(3)} + C_{\ell\ell} + C_{Hq}^{(3)} - C_{H\ell}^{(3)} \right). \tag{D.3}$$

E   Global Fit results

Considering now all the observables listed, a total 103 observables, the global fit result using the method described in Section 2.2 is given as follows. In the global fit $r = 19 = \dim\{C_G\}$ once the auxiliary conditions are imposed. Since our observables are shifted linearly in the Wilson coefficients, the Cramer-Rao bound is exact, meaning that the covariance matrix of our Wilson coefficients V_{C_G} is exactly given by $V_{C_G} = \mathcal{I}^{-1}$. We give the Fisher information matrix as $\mathcal{I}_{\Delta_{SMEFT}}$. Note that we have not included exclusive measurements of W pair production in this version of the fit. This is due to the severe challenge of properly incorporating these measurements in the SMEFT. Some of these challenges are discussed in Ref. [20]. When these measurements are included, it is expected that the flat directions will be lifted, and the degree

---

[19]Note this point was first stressed in the context of SUSY in Ref.[98].

of constraint will be in between the results shown in Figures 6-8. The ordering of the rows and columns of the Fisher matrix corresponds to the Wilson coefficient order in C_G. We give the $C_{G,min}$ for $\Delta_{SMEFT} = \{0, 0.1\%, 0.3\%, 0.5\%, 1\%\}$ in Table 1.

$$\mathcal{I}_0 = 10^6 \times \begin{bmatrix}
7.73 & 0.668 & -0.236 & -7.83 & -5.73 & 0.189 & 3.75 & 0.343 & -3.83 & -0.248 & -0.0371 & 0.0898 & -0.0768 & 0.00172 & 0.0421 & -0.0222 & -0.0386 & -0.357 & -0.0106 \\
 & 5.94 & 2.17 & -0.79 & -3.77 & -27.8 & 1.92 & 1.71 & -3.55 & -0.851 & 0 & -0.00587 & 0.0296 & 0 & -0.0133 & -0.0133 & -0.0157 & 0.0697 & 0.0285 \\
 & & 1.01 & 0.8 & -0.245 & -11.3 & -0.444 & 0.359 & -1.33 & -0.181 & 0 & 0.0296 & 0.00618 & 0.0534 & -0.0133 & -0.0193 & -0.0412 & -0.0558 & 0.0321 \\
 & & & 16.4 & 3.69 & -2.42 & -6.23 & 3.44 & -4.89 & -1.59 & 0.131 & -0.163 & 0.132 & -0.04 & -0.0921 & 0.0552 & 0.0487 & 0.678 & 0.0106 \\
 & & & & 29.4 & 10.3 & -20.1 & -19.9 & 17.8 & 6.97 & -0.0692 & 0.259 & -0.187 & 0 & 0.0904 & -0.0764 & -0.157 & 10.2 & 0.00868 \\
 & & & & & 138 & -2.12 & -5.93 & 15.8 & 2.96 & 0 & -0.0151 & 0.0649 & 0.062 & -0.0429 & -0.0207 & -0.034 & 0.155 & 0.0606 \\
 & & & & & & 18.8 & 14 & -2.6 & -1.47 & 0.227 & -0.159 & 0.122 & -0.077 & -0.0626 & 0.0441 & 0.0856 & -10.6 & 0.00357 \\
 & & & & & & & 17.7 & -11.3 & -4.43 & -0.133 & -0.211 & 0.159 & -0.0229 & -0.0807 & 0.0601 & 0.117 & -10.4 & 0.000977 \\
 & & & & & & & & 29.3 & 10.6 & -0.05 & 0.194 & -0.124 & 0.0136 & 0.0536 & -0.0622 & -0.139 & -0.653 & 0.0236 \\
 & & & & & & & & & 4.66 & 0.168 & 0.106 & -0.0797 & 0 & 0.0296 & -0.0243 & -0.0727 & -0.369 & -0.000488 \\
 & & & & & & & & & & & 0.102 & 0 & 0.11 & 0.0221 & -0.0417 & -0.0734 & -0.332 & 0 \\
 & & & & & & & & & & & & -0.0512 & & -0.0417 & 0.00293 & 0.00151 & 0.246 & 0.0285 \\
 & & & & & & & & & & & & 0.0668 & & 0.0357 & 0.000263 & 0.0133 & -0.133 & 0.0321 \\
 & & & & & & & & & & & & & & & 0.0272 & 0.0441 & 0.103 & 0 \\
 & & & & & & & & & & & & & & & & 0.0874 & 0.166 & -0.0285 \\
 & & & & & & & & & & & & & & & & & 12.4 & -0.0321 \\
 & & & & & & & & & & & & & & & & & & -0.0606 \\
 & & & & & & & & & & & & & & & & & & -0.00358 \\
 & & & & & & & & & & & & & & & & & & 0.0606
\end{bmatrix} \tag{E.1}$$

$$\mathcal{I}_{0.1} = 10^6 \times \begin{bmatrix}
4.48 & 0.409 & -0.0584 & -2.69 & -4.28 & -0.24 & 1.97 & 1.29 & -4.45 & -0.704 & -0.037 & 0.0896 & -0.0766 & 0.00174 & 0.042 & -0.0221 & -0.0385 & -0.356 & -0.0106 \\
 & 5.46 & 2.06 & -0.364 & -3.05 & -25.9 & 1.39 & 1.46 & -3.2 & -0.739 & 0 & -0.00583 & 0.0295 & 0 & -0.0133 & -0.0133 & -0.0158 & 0.0695 & 0.0285 \\
 & & 0.911 & 0.468 & -0.56 & -10.4 & -0.119 & 0.431 & -1.31 & -0.21 & 0 & 0.0295 & 0.00619 & 0.0534 & -0.0133 & -0.0193 & -0.0411 & -0.0556 & 0.0321 \\
 & & & 7.97 & 1.09 & -1.49 & -3.15 & 2.16 & -3.97 & -0.943 & 0.131 & -0.163 & 0.131 & -0.0399 & -0.0917 & 0.055 & 0.0488 & 0.675 & 0.0106 \\
 & & & & 13.3 & 10.4 & -8.24 & -8.34 & 9.7 & 2.86 & -0.0692 & 0.259 & -0.186 & 0 & 0.0902 & -0.0762 & -0.157 & 2.02 & 0.00867 \\
 & & & & & 128 & -2.75 & -5.74 & 14.8 & 2.86 & 0 & -0.015 & 0.0647 & 0.0619 & -0.0429 & -0.0207 & -0.0341 & 0.155 & 0.0606 \\
 & & & & & & 7.3 & 4.77 & -1.81 & -0.931 & 0.226 & -0.158 & 0.122 & -0.0769 & -0.0625 & 0.044 & 0.0852 & -2.36 & 0.00357 \\
 & & & & & & & 7.2 & -6.89 & -2.07 & -0.133 & -0.211 & 0.159 & -0.0229 & -0.0805 & 0.06 & 0.117 & -2.17 & 0.000976 \\
 & & & & & & & & 15.2 & 3.72 & -0.05 & 0.193 & -0.124 & 0.0135 & 0.0535 & -0.0621 & -0.138 & -0.652 & 0.0236 \\
 & & & & & & & & & 1.18 & 0.168 & 0.105 & -0.0794 & 0 & 0.0297 & -0.0243 & -0.0722 & -0.369 & -0.000488 \\
 & & & & & & & & & & & 0.102 & 0 & 0.11 & 0.022 & -0.0416 & -0.0732 & -0.331 & 0 \\
 & & & & & & & & & & & & -0.051 & & -0.0416 & 0.00289 & 0.00144 & 0.245 & 0.0285 \\
 & & & & & & & & & & & & 0.0666 & & 0.0356 & 0.000294 & 0.0133 & -0.133 & 0.0321 \\
 & & & & & & & & & & & & & & & 0.0272 & 0.044 & 0.103 & 0 \\
 & & & & & & & & & & & & & & & & 0.0872 & 0.165 & -0.0285 \\
 & & & & & & & & & & & & & & & & & 4.2 & -0.0321 \\
 & & & & & & & & & & & & & & & & & & -0.0606 \\
 & & & & & & & & & & & & & & & & & & -0.00357 \\
 & & & & & & & & & & & & & & & & & & 0.0606
\end{bmatrix} \tag{E.2}$$

$$
\mathcal{I}_{0.3} = 10^6 \times
\begin{bmatrix}
2.46 & 0.113 & 0.0892 & 0.39 & -2.62 & -0.406 & 0.306 & 1.5 & -4.45 & -0.805 & -0.0363 & 0.0874 & -0.0749 & 0.00187 & 0.0411 & -0.0215 & -0.0375 & -0.348 & -0.0105 \\
 & 3.7 & 1.44 & -0.0215 & -1.79 & -17.7 & 0.708 & 0.913 & -2.08 & -0.466 & 0 & -0.00552 & 0.029 & 0 & -0.0132 & -0.0132 & -0.016 & 0.0682 & 0.0282 \\
 & & 0.609 & 0.156 & -0.605 & -7.04 & 0.101 & 0.361 & -0.973 & -0.175 & 0.13 & 0.029 & 0.00626 & 0.0529 & -0.0132 & -0.0191 & -0.0404 & -0.0545 & 0.0317 \\
 & & & 2.84 & -1.55 & -0.482 & -0.413 & 1.94 & -0.842 & -0.842 & -0.0689 & -0.159 & 0.128 & -0.0397 & -0.0885 & 0.053 & 0.0498 & 0.656 & 0.0105 \\
 & & & & 6.36 & 7.56 & -2.19 & -4.34 & 8.02 & 2.04 & 0 & 0.253 & -0.182 & 0 & 0.0888 & -0.0749 & -0.152 & -0.482 & 0.00858 \\
 & & & & & 87.3 & -2.36 & -3.97 & 10 & 1.97 & 0 & -0.0143 & 0.0637 & 0 & -0.0424 & -0.0205 & -0.0344 & 0.152 & 0.0599 \\
 & & & & & & 1.69 & 1.27 & -0.965 & -0.438 & 0.224 & -0.155 & 0.119 & 0.0611 & -0.0613 & 0.0431 & 0.0828 & 0.151 & 0.00353 \\
 & & & & & & & 3.69 & -5.93 & -1.53 & -0.133 & -0.206 & 0.155 & -0.0764 & -0.079 & 0.0588 & 0.113 & 0.335 & 0.000966 \\
 & & & & & & & & 13.6 & 3.08 & -0.0497 & 0.189 & -0.121 & -0.0227 & 0.053 & -0.0613 & -0.133 & -0.639 & 0.0233 \\
 & & & & & & & & & 0.833 & 0.167 & 0.103 & -0.0776 & 0.0132 & 0.0297 & -0.0241 & -0.0691 & -0.362 & -0.000483 \\
 & & & & & & & & & & 0.0132 & 0 & 0 & 0 & 0.0212 & -0.0408 & -0.0718 & -0.323 & 0.0282 \\
 & & & & & & & & & & & 0.0992 & -0.0495 & 0 & -0.0408 & 0.00256 & 0.000948 & 0.239 & 0.0317 \\
 & & & & & & & & & & & & 0.0652 & 0 & 0 & 0.000521 & 0.0132 & -0.129 & -0.0282 \\
 & & & & & & & & & & & & & 0.109 & 0 & 0.0267 & 0.0435 & 0.0998 & -0.0317 \\
 & & & & & & & & & & & & & & 0.0349 & 0 & 0 & 0.162 & -0.0599 \\
 & & & & & & & & & & & & & & & 0.0267 & 0 & 0 & -0.00354 \\
 & & & & & & & & & & & & & & & & 0.0856 & 0 & 0 \\
 & & & & & & & & & & & & & & & & & 1.64 & 0 \\
 & & & & & & & & & & & & & & & & & & 0.0599
\end{bmatrix}
\tag{E.3}
$$

$$
\mathcal{I}_{0.5} = 10^6 \times
\begin{bmatrix}
2.12 & 0.0335 & 0.0976 & 0.805 & -2.26 & -0.29 & 0.0225 & 1.46 & -4.3 & -0.785 & -0.0351 & 0.0836 & -0.0718 & 0.00212 & 0.0394 & -0.0205 & -0.0357 & -0.333 & -0.0103 \\
 & 2.61 & 1.02 & 0.0134 & -1.21 & -12.5 & 0.47 & 0.626 & -1.42 & -0.321 & 0 & -0.00498 & 0.0281 & 0 & -0.0129 & -0.013 & -0.0162 & 0.0656 & 0.0276 \\
 & & 0.433 & 0.0925 & -0.464 & -4.94 & 0.0913 & 0.268 & -0.719 & -0.13 & 0.128 & 0.0281 & 0.00638 & 0.052 & -0.013 & -0.0186 & -0.0393 & -0.0525 & 0.0311 \\
 & & & 2.04 & -1.94 & -0.208 & 0.0315 & 1.89 & -3.68 & -0.833 & -0.0684 & -0.152 & 0.123 & -0.0392 & -0.0834 & 0.0497 & 0.0504 & 0.623 & 0.0103 \\
 & & & & 5.07 & 5.3 & -1.25 & -3.66 & 7.36 & 1.82 & 0 & 0.242 & -0.174 & 0 & 0.0858 & -0.0723 & -0.144 & -0.717 & 0.0587 \\
 & & & & & 61.5 & -1.71 & -2.73 & 6.92 & 1.35 & 0 & -0.0131 & 0.0617 & 0 & -0.0415 & -0.0202 & -0.0347 & 0.146 & 0.00346 \\
 & & & & & & 0.872 & 0.791 & -0.733 & -0.333 & 0.22 & -0.148 & 0.114 & 0.0596 & -0.059 & 0.0414 & 0.0786 & 0.398 & 0.000947 \\
 & & & & & & & 3.16 & -5.53 & -1.4 & -0.132 & -0.197 & 0.148 & -0.0755 & -0.076 & 0.0564 & 0.108 & 0.574 & 0.0229 \\
 & & & & & & & & 12.8 & 2.86 & -0.0491 & 0.181 & -0.115 & -0.0223 & 0.0516 & -0.0596 & -0.126 & -0.615 & -0.000473 \\
 & & & & & & & & & 0.749 & 0.164 & 0.0984 & -0.0742 & 0.0125 & 0.0293 & -0.0236 & -0.0643 & -0.35 & 0 \\
 & & & & & & & & & & 0.0125 & 0 & 0 & 0 & 0.0199 & -0.0393 & -0.0692 & -0.308 & 0.0276 \\
 & & & & & & & & & & & 0.095 & -0.0469 & 0 & -0.0393 & 0.002 & 9.4e{-}05 & 0.228 & 0.0311 \\
 & & & & & & & & & & & & 0.0626 & 0 & 0 & 0.000872 & 0.0131 & -0.123 & -0.0276 \\
 & & & & & & & & & & & & & 0.108 & 0 & 0 & 0.0425 & 0.0951 & -0.0311 \\
 & & & & & & & & & & & & & & 0.0337 & 0 & 0 & 0.155 & -0.0587 \\
 & & & & & & & & & & & & & & & 0.0259 & 0 & 0 & -0.00347 \\
 & & & & & & & & & & & & & & & & 0.0828 & 0 & 0 \\
 & & & & & & & & & & & & & & & & & 1.32 & 0 \\
 & & & & & & & & & & & & & & & & & & 0.0587
\end{bmatrix}
\tag{E.4}
$$

$$
\mathcal{I}_{1.0} = 10^6 \times
\begin{bmatrix}
1.78 & -0.0231 & 0.0767 & 0.908 & -1.91 & -0.132 & -0.0948 & 1.31 & -3.86 & -0.708 & -0.0299 & 0.0703 & -0.0611 & 0.00305 & 0.0335 & -0.0168 & -0.0295 & -0.282 & -0.00942 \\
- & 1.54 & 0.601 & 0.0121 & -0.668 & -7.34 & 0.27 & 0.348 & -0.766 & -0.18 & 0 & -0.00328 & 0.0248 & 0 & -0.0113 & -0.0122 & -0.0159 & 0.0561 & 0.0253 \\
- & - & 0.261 & 0.0462 & -0.285 & -2.89 & 0.0578 & 0.161 & -0.437 & -0.077 & 0 & 0.0248 & 0.00656 & 0.0481 & -0.0122 & -0.0168 & -0.0352 & -0.0449 & 0.0285 \\
- & - & - & 1.5 & -1.94 & -0.0138 & 0.208 & 1.7 & -3.33 & -0.772 & 0.12 & -0.128 & 0.104 & -0.037 & -0.0686 & 0.0403 & 0.0469 & 0.519 & 0.00943 \\
- & - & - & - & 3.98 & 3.02 & -0.709 & -2.99 & 6.29 & 1.52 & -0.0663 & 0.204 & -0.146 & 0 & 0.0737 & -0.0621 & -0.119 & -0.704 & 0.0077 \\
- & - & - & - & - & 36.2 & -1.01 & -1.51 & 3.88 & 0.747 & 0 & -0.00906 & 0.0543 & 0 & -0.0373 & -0.0191 & -0.0342 & 0.124 & 0.0538 \\
- & - & - & - & - & - & 0.44 & 0.503 & -0.518 & -0.241 & 0.202 & -0.125 & 0.0964 & 0.0536 & -0.0504 & 0.035 & 0.0652 & 0.431 & 0.00317 \\
- & - & - & - & - & - & - & 2.62 & -4.79 & -1.19 & -0.128 & -0.166 & 0.125 & -0.0714 & -0.0648 & 0.0479 & 0.0895 & 0.581 & 0.000868 \\
- & - & - & - & - & - & - & - & 11.1 & 2.46 & -0.0465 & 0.153 & -0.0965 & -0.0208 & 0.0448 & -0.0522 & -0.105 & -0.525 & 0.0209 \\
- & - & - & - & - & - & - & - & - & 0.624 & 0.153 & 0.083 & -0.0627 & -0.00988 & 0.026 & -0.0206 & -0.0511 & -0.3 & -0.000434 \\
- & - & - & - & - & - & - & - & - & - & 0 & 0 & 0 & 0 & 0 & 0 & 0 & 0 & 0 \\
- & - & - & - & - & - & - & - & - & - & - & 0.0802 & -0.0378 & 0.103 & 0.0154 & -0.0339 & -0.06 & -0.257 & 0.0253 \\
- & - & - & - & - & - & - & - & - & - & - & - & 0.0535 & 0 & -0.0339 & 0.000257 & -0.00244 & 0.19 & 0.0285 \\
- & - & - & - & - & - & - & - & - & - & - & - & - & 0.103 & 0 & 0 & 0 & 0 & 0 \\
- & - & - & - & - & - & - & - & - & - & - & - & - & - & 0.0297 & 0.00169 & 0.0128 & -0.101 & -0.0253 \\
- & - & - & - & - & - & - & - & - & - & - & - & - & - & - & 0.0231 & 0.0381 & 0.0788 & -0.0285 \\
- & - & - & - & - & - & - & - & - & - & - & - & - & - & - & - & 0.0732 & 0.131 & -0.0538 \\
- & - & - & - & - & - & - & - & - & - & - & - & - & - & - & - & - & 1 & -0.00317 \\
- & - & - & - & - & - & - & - & - & - & - & - & - & - & - & - & - & - & 0.0538
\end{bmatrix}
\tag{E.5}
$$

References

[1] B. Grinstein and M. Trott, *A Higgs-Higgs bound state due to new physics at a TeV*, *Phys.Rev.* **D76** (2007) 073002, [arXiv:0704.1505].

[2] S. Weinberg, *Baryon and Lepton Nonconserving Processes*, *Phys.Rev.Lett.* **43** (1979) 1566–1570.

[3] W. Buchmuller and D. Wyler, *Effective Lagrangian Analysis of New Interactions and Flavor Conservation*, *Nucl.Phys.* **B268** (1986) 621–653.

[4] B. Grzadkowski, M. Iskrzynski, M. Misiak, and J. Rosiek, *Dimension-Six Terms in the Standard Model Lagrangian*, *JHEP* **1010** (2010) 085, [arXiv:1008.4884].

[5] L. Abbott and M. B. Wise, *The Effective Hamiltonian for Nucleon Decay*, *Phys.Rev.* **D22** (1980) 2208.

[6] L. Lehman, *Extending the Standard Model Effective Field Theory with the Complete Set of Dimension-7 Operators*, *Phys.Rev.* **D90** (2014), no. 12 125023, [arXiv:1410.4193].

[7] L. Lehman and A. Martin, *Low-derivative operators of the Standard Model effective field theory via Hilbert series methods*, arXiv:1510.00372.

[8] M. Ciuchini, E. Franco, S. Mishima, and L. Silvestrini, *Electroweak Precision Observables, New Physics and the Nature of a 126 GeV Higgs Boson*, *JHEP* **1308** (2013) 106, [arXiv:1306.4644].

[9] M. Ciuchini, E. Franco, S. Mishima, M. Pierini, L. Reina, et al., *Update of the electroweak precision fit, interplay with Higgs-boson signal strengths and model-independent constraints on new physics*, arXiv:1410.6940.

[10] **Gfitter Group** Collaboration, M. Baak et al., *The global electroweak fit at NNLO and prospects for the LHC and ILC*, *Eur.Phys.J.* **C74** (2014), no. 9 3046, [arXiv:1407.3792].

[11] G. Durieux, F. Maltoni, and C. Zhang, *Global approach to top-quark flavor-changing interactions*, *Phys. Rev.* **D91** (2015), no. 7 074017, [arXiv:1412.7166].

[12] A. A. Petrov, S. Pokorski, J. D. Wells, and Z. Zhang, *Role of low-energy observables in precision Higgs boson analyses*, *Phys. Rev.* **D91** (2015), no. 7 073001, [arXiv:1501.02803].

[13] *Determining Triple Gauge Boson Couplings from Higgs Data*, *Phys.Rev.Lett.* **111** (2013) 011801, [arXiv:1304.1151].

[14] B. Batell, S. Gori, and L.-T. Wang, *Higgs Couplings and Precision Electroweak Data*, *JHEP* **01** (2013) 139, [arXiv:1209.6382].

[15] *Searching for New Physics in the Three-Body Decays of the Higgs-like Particle*, *JHEP* **10** (2013) 077, [arXiv:1305.6938].

[16] A. Pomarol and F. Riva, *Towards the Ultimate SM Fit to Close in on Higgs Physics*, *JHEP* **01** (2014) 151, [arXiv:1308.2803].

[17] J. D. Wells and Z. Zhang, *Precision Electroweak Analysis after the Higgs Boson Discovery*, *Phys.Rev.* **D90** (2014), no. 3 033006, [arXiv:1406.6070].

[18] J. Ellis, V. Sanz, and T. You, *Complete Higgs Sector Constraints on Dimension-6 Operators*, *JHEP* **1407** (2014) 036, [arXiv:1404.3667].

[19] J. Ellis, V. Sanz, and T. You, *The Effective Standard Model after LHC Run I*, *JHEP* **03** (2015) 157, [arXiv:1410.7703].

[20] M. Trott, *On the consistent use of Constructed Observables*, *JHEP* **02** (2015) 046, [arXiv:1409.7605].

[21] B. Henning, X. Lu, and H. Murayama, *How to use the Standard Model effective field theory*, arXiv:1412.1837.

[22] A. Falkowski and F. Riva, *Model-independent precision constraints on dimension-6 operators*, *JHEP* **02** (2015) 039, [arXiv:1411.0669].

[23] J. de Blas, M. Chala, and J. Santiago, *Renormalization Group Constraints on New Top Interactions from Electroweak Precision Data*, arXiv:1507.00757.

[24] J. D. Wells and Z. Zhang, *Status and prospects of precision analyses with $e^+e^- \to W^+W^-$*, arXiv:1507.01594.

[25] S. Banerjee, T. Mandal, B. Mellado, and B. Mukhopadhyaya, *Cornering dimension-6 HVV interactions at high luminosity LHC: the role of event ratios*, *JHEP* **09** (2015) 057, [arXiv:1505.00226].

[26] L. Berthier and M. Trott, *Towards consistent Electroweak Precision Data constraints in the SMEFT*, *JHEP* **05** (2015) 024, [arXiv:1502.02570].

[27] B. Grinstein and M. B. Wise, *Operator analysis for precision electroweak physics*, *Phys.Lett.* **B265** (1991) 326–334.

[28] Z. Han and W. Skiba, *Effective theory analysis of precision electroweak data*, *Phys.Rev.* **D71** (2005) 075009, [hep-ph/0412166].

[29] R. Alonso, E. E. Jenkins, A. V. Manohar, and M. Trott, *Renormalization Group Evolution of the Standard Model Dimension Six Operators III: Gauge Coupling Dependence and Phenomenology*, *JHEP* **1404** (2014) 159, [arXiv:1312.2014].

[30] A. Efrati, A. Falkowski, and Y. Soreq, *Electroweak constraints on flavorful effective theories*, *JHEP* **07** (2015) 018, [arXiv:1503.07872].

[31] A. Freitas, *Higher-order electroweak corrections to the partial widths and branching ratios of the Z boson*, *JHEP* **1404** (2014) 070, [arXiv:1401.2447].

[32] **Particle Data Group** Collaboration, K. Olive et al., *Review of Particle Physics*, *Chin.Phys.* **C38** (2014) 090001.

[33] **Two Fermion Working Group** Collaboration, M. Kobel et al., *Two-Fermion Production in Electron-Positron Collisions*, hep-ph/0007180.

[34] **TOPAZ** Collaboration, Y. Inoue et al., *Measurement of the cross-section and forward - backward charge asymmetry for the b and c quark in e+ e- annihilation with inclusive muons at s**(1/2) = 58-GeV*, *Eur. Phys. J.* **C18** (2000) 273–282, [hep-ex/0012033].

[35] **NuTeV** Collaboration, G. Zeller et al., *A Precise determination of electroweak parameters in neutrino nucleon scattering*, *Phys.Rev.Lett.* **88** (2002) 091802, [hep-ex/0110059].

[36] D. Yennie, S. C. Frautschi, and H. Suura, *The infrared divergence phenomena and high-energy processes*, *Annals Phys.* **13** (1961) 379–452.

[37] M. Greco, *Structure Functions and Initial Final State Interference in QED*, *Phys.Lett.* **B240** (1990) 219–223.

[38] E. E. Jenkins, A. V. Manohar, and M. Trott, *Renormalization Group Evolution of the Standard Model Dimension Six Operators I: Formalism and lambda Dependence*, *JHEP* **1310** (2013) 087, [arXiv:1308.2627].

[39] E. E. Jenkins, A. V. Manohar, and M. Trott, *Renormalization Group Evolution of the Standard Model Dimension Six Operators II: Yukawa Dependence*, *JHEP* **1401** (2014) 035, [arXiv:1310.4838].

[40] C. Hartmann and M. Trott, *On one-loop corrections in the standard model effective field theory; the $\Gamma(h \to \gamma\gamma)$ case*, *JHEP* **07** (2015) 151, [arXiv:1505.02646].

[41] M. Ghezzi, R. Gomez-Ambrosio, G. Passarino, and S. Uccirati, *NLO Higgs effective field theory and $\hat{I}\check{z}$-framework*, *JHEP* **07** (2015) 175, [arXiv:1505.03706].

[42] C. Hartmann and M. Trott, *Higgs decay to two photons at one-loop in the SMEFT*, arXiv:1507.03568.

[43] R. Alonso, B. Grinstein, and J. Martin Camalich, *$SU(2) \times U(1)$ gauge invariance and the shape of new physics in rare B decays*, *Phys. Rev. Lett.* **113** (2014) 241802, [arXiv:1407.7044].

[44] A. David and G. Passarino, *Through precision straits to next standard model heights*, arXiv:1510.00414.

[45] D. C. Kennedy and B. W. Lynn, *Electroweak Radiative Corrections with an Effective Lagrangian: Four Fermion Processes*, *Nucl. Phys.* **B322** (1989) 1.

[46] M. E. Peskin and T. Takeuchi, *Estimation of oblique electroweak corrections*, *Phys.Rev.* **D46** (1992) 381–409.

[47] M. Golden and L. Randall, *Radiative Corrections to Electroweak Parameters in Technicolor Theories*, *Nucl.Phys.* **B361** (1991) 3–23.

[48] B. Holdom and J. Terning, *Large corrections to electroweak parameters in technicolor theories*, *Phys.Lett.* **B247** (1990) 88–92.

[49] C. Grojean, W. Skiba, and J. Terning, *Disguising the oblique parameters*, *Phys. Rev.* **D73** (2006) 075008, [hep-ph/0602154].

[50] V. Cirigliano, J. Jenkins, and M. Gonzalez-Alonso, *Semileptonic decays of light quarks beyond the Standard Model*, *Nucl. Phys.* **B830** (2010) 95–115, [arXiv:0908.1754].

[51] **ALEPH, DELPHI, L3, OPAL, LEP Electroweak** Collaboration, S. Schael et al., *Electroweak Measurements in Electron-Positron Collisions at W-Boson-Pair Energies at LEP*, *Phys.Rept.* **532** (2013) 119–244, [arXiv:1302.3415].

[52] A. Arbuzov, M. Awramik, M. Czakon, A. Freitas, M. Grunewald, et al., *ZFITTER: A Semi-analytical program for fermion pair production in e+ e- annihilation, from version 6.21 to version 6.42*, *Comput.Phys.Commun.* **174** (2006) 728–758, [hep-ph/0507146].

[53] **AMY** Collaboration, C. Velissaris et al., *Measurements of cross-section and charge asymmetry for e+ e- —> mu+ mu- and e+ e- —> tau+ tau- at s**(1/2) = 57.8-GeV*, *Phys.Lett.* **B331** (1994) 227–235.

[54] **VENUS** Collaboration, M. Miura et al., *Precise measurement of the e+ e- —> mu+ mu- reaction at s**(1/2) = 57.77-GeV*, *Phys.Rev.* **D57** (1998) 5345–5362.

[55] **JADE** Collaboration, S. Hegner et al., *Final Results on μ and Tau Pair Production by the Jade Collaboration at PETRA*, *Z.Phys.* **C46** (1990) 547–554.

[56] M. Derrick, E. Fernandez, R. Fries, L. Hyman, P. Kooijman, et al., *New Results on the Reaction $e^+e^- \to \mu^+\mu^-$ at $\sqrt{s} = 29$-GeV*, *Phys.Rev.* **D31** (1985) 2352.

[57] **HRS Collaboration** Collaboration, S. Abachi et al., *Production Cross-section and Topological Decay Branching Fractions of the τ Lepton*, *Phys.Rev.* **D40** (1989) 902.

[58] H. Sagawa, T. Tauchi, M. Tanabashi, and S. Uehara, *TRISTAN physics at high luminosities. Proceedings, 3rd Workshop, Tsukuba, Japan, November 16-18, 1994*, .

[59] T. ALEPH, DELPHI, L3, OPAL, S. Collaborations, the LEP Electroweak Working Group, the SLD Electroweak, and H. F. Groups, *Precision Electroweak Measurements on the Z Resonance*, *Phys. Rept.* **427** (2006) 257, [`hep-ex/0509008`].

[60] P. J. Mohr, B. N. Taylor, and D. B. Newell, *CODATA Recommended Values of the Fundamental Physical Constants: 2010*, *Rev. Mod. Phys.* **84** (2012) 1527–1605, [`arXiv:1203.5425`].

[61] **ATLAS, CMS** Collaboration, G. Aad et al., *Combined Measurement of the Higgs Boson Mass in pp Collisions at $\sqrt{s} = 7$ and 8 TeV with the ATLAS and CMS Experiments*, *Phys. Rev. Lett.* **114** (2015) 191803, [`arXiv:1503.07589`].

[62] **CDF Collaboration, D0 Collaboration** Collaboration, T. E. W. Group, *2012 Update of the Combination of CDF and D0 Results for the Mass of the W Boson*, `arXiv:1204.0042`.

[63] M. Awramik, M. Czakon, A. Freitas, and G. Weiglein, *Precise prediction for the W boson mass in the standard model*, *Phys.Rev.* **D69** (2004) 053006, [`hep-ph/0311148`].

[64] M. Awramik, M. Czakon, and A. Freitas, *Electroweak two-loop corrections to the effective weak mixing angle*, *JHEP* **11** (2006) 048, [`hep-ph/0608099`].

[65] *http://www.slac.stanford.edu/cgi-wrap/getdoc/ssi90-019.pdf*, .

[66] **VENUS** Collaboration, K. Abe et al., *A Study of the charm and bottom quark production in e+ e- annihilation at s**(1/2) = 58-GeV using prompt electrons*, *Phys.Lett.* **B313** (1993) 288–298.

[67] K. K. Gan et al., *Measurement of the Reaction $e^+e^- \to \tau^+\tau^-$ at $\sqrt{s} = 29$-GeV*, *Phys. Lett.* **B153** (1985) 116.

[68] H. Bhabba, *The Scattering of Positrons by Electrons with Exchange on Diracs Theory of the Positron*, *Proc.Roy. Soc* **A154** (1936) 195.

[69] S. Jadach, W. Placzek, and B. F. L. Ward, *BHWIDE 1.00: O(alpha) YFS exponentiated Monte Carlo for Bhabha scattering at wide angles for LEP-1 / SLC and LEP-2*, *Phys. Lett.* **B390** (1997) 298–308, [`hep-ph/9608412`].

[70] S. Jadach, B. F. L. Ward, and Z. Was, *Coherent exclusive exponentiation for precision Monte Carlo calculations*, *Phys. Rev.* **D63** (2001) 113009, [`hep-ph/0006359`].

[71] **CHARM Collaboration** Collaboration, J. Allaby et al., *A Precise Determination of the Electroweak Mixing Angle from Semileptonic Neutrino Scattering*, *Z.Phys.* **C36** (1987) 611.

[72] **CHARM-II Collaboration** Collaboration, P. Vilain et al., *Precision measurement of electroweak parameters from the scattering of muon-neutrinos on electrons*, *Phys.Lett.* **B335** (1994) 246–252.

[73] L. A. Ahrens et al., *Determination of electroweak parameters from the elastic scattering of muon-neutrinos and anti-neutrinos on electrons*, Phys. Rev. **D41** (1990) 3297–3316.

[74] H. Abramowicz, R. Belusevic, A. Blondel, H. Blumer, P. Bockmann, et al., *A Precision Measurement of sin**2theta(W) from Semileptonic Neutrino Scattering*, Phys.Rev.Lett. **57** (1986) 298.

[75] **CCFR, E744, E770** Collaboration, K. S. McFarland et al., *A Precision measurement of electroweak parameters in neutrino - nucleon scattering*, Eur.Phys.J. **C1** (1998) 509–513, [`hep-ex/9701010`].

[76] **SLAC E158 Collaboration** Collaboration, P. Anthony et al., *Precision measurement of the weak mixing angle in Moller scattering*, Phys.Rev.Lett. **95** (2005) 081601, [`hep-ex/0504049`].

[77] C. Prescott, W. Atwood, R. L. Cottrell, H. DeStaebler, E. L. Garwin, et al., *Further Measurements of Parity Nonconservation in Inelastic electron Scattering*, Phys.Lett. **B84** (1979) 524.

[78] E. Beise, M. Pitt, and D. Spayde, *The SAMPLE experiment and weak nucleon structure*, Prog.Part.Nucl.Phys. **54** (2005) 289–350, [`nucl-ex/0412054`].

[79] **CHARM** Collaboration, J. Dorenbosch et al., *EXPERIMENTAL RESULTS ON NEUTRINO - ELECTRON SCATTERING*, Z. Phys. **C41** (1989) 567. [Erratum: Z. Phys.C51,142(1991)].

[80] J. Erler and S. Su, *The Weak Neutral Current*, Prog.Part.Nucl.Phys. **71** (2013) 119–149, [`arXiv:1303.5522`].

[81] C. H. Llewellyn Smith, *On the Determination of sin**2-Theta-w in Semileptonic Neutrino Interactions*, Nucl. Phys. **B228** (1983) 205.

[82] A. D. Martin, R. G. Roberts, W. J. Stirling, and R. S. Thorne, *Uncertainties of predictions from parton distributions. 2. Theoretical errors*, Eur. Phys. J. **C35** (2004) 325–348, [`hep-ph/0308087`].

[83] C. F. V. Weizsacker, *Zur Theorie der Kernmassen*, Z. Phys. **96** (1935) 431–458.

[84] E. J. Williams, *Nature of the high-energy particles of penetrating radiation and status of ionization and radiation formulae*, Phys. Rev. **45** (1934) 729–730.

[85] W. Altmannshofer, S. Gori, M. Pospelov, and I. Yavin, *Quark flavor transitions in $L_\mu - L_\tau$ models*, Phys. Rev. **D89** (2014) 095033, [`arXiv:1403.1269`].

[86] W. Altmannshofer, S. Gori, M. Pospelov, and I. Yavin, *Neutrino Trident Production: A Powerful Probe of New Physics with Neutrino Beams*, Phys. Rev. Lett. **113** (2014) 091801, [`arXiv:1406.2332`].

[87] R. W. Brown, R. H. Hobbs, J. Smith, and N. Stanko, *Intermediate boson. iii. virtual-boson effects in neutrino trident production*, Phys. Rev. D **6** (Dec, 1972) 3273–3292.

[88] R. Belusevic and J. Smith, *W - z interference in ν -nucleus scattering*, Phys. Rev. D **37** (May, 1988) 2419–2422.

[89] **CHARM-II** Collaboration, D. Geiregat et al., *First observation of neutrino trident production*, Phys. Lett. **B245** (1990) 271–275.

[90] S. R. e. a. Mishra, *Neutrino tridents and W - Z interference*, Phys. Rev. Lett. **66** (Jun, 1991) 3117–3120.

[91] P. G. Blunden, W. Melnitchouk, and A. W. Thomas, $\gamma - Z$ *box corrections to weak charges of heavy nuclei in atomic parity violation*, Phys. Rev. Lett. **109** (2012) 262301, [arXiv:1208.4310].

[92] P. Vetter, D. Meekhof, P. Majumder, S. Lamoreaux, and E. Fortson, *Precise test of electroweak theory from a new measurement of parity nonconservation in atomic thallium*, Phys.Rev.Lett. **74** (1995) 2658–2661.

[93] C. Wood, S. Bennett, D. Cho, B. Masterson, J. Roberts, et al., *Measurement of parity nonconservation and an anapole moment in cesium*, Science **275** (1997) 1759–1763.

[94] A. Derevianko, *Reconciliation of the measurement of parity nonconservation in Cs with the standard model*, Phys.Rev.Lett. **85** (2000) 1618–1621, [hep-ph/0005274].

[95] **SAMPLE** Collaboration, T. Ito et al., *Parity violating electron deuteron scattering and the proton's neutral weak axial vector form-factor*, Phys.Rev.Lett. **92** (2004) 102003, [nucl-ex/0310001].

[96] **HAPPEX** Collaboration, A. Acha et al., *Precision Measurements of the Nucleon Strange Form Factors at Q**2 ~ 0.1-GeV**2*, Phys.Rev.Lett. **98** (2007) 032301, [nucl-ex/0609002].

[97] E. Derman and W. J. Marciano, *Parity Violating Asymmetries in Polarized Electron Scattering*, Annals Phys. **121** (1979) 147.

[98] R. Barbieri, C. Bouchiat, A. Georges, and P. Le Doussal, *Limits on Superparticle Masses From Quark - Lepton Universality*, Nucl. Phys. **B269** (1986) 253.

[99] **FlaviaNet Working Group on Kaon Decays** Collaboration, M. Antonelli et al., *An Evaluation of Vus and precise tests of the Standard Model from world data on leptonic and semileptonic kaon decays*, Eur. Phys. J. **C69** (2010) 399–424, [arXiv:1005.2323].

$1:X^3$	
Q_G	$f^{ABC}G_\mu^{A\nu}G_\nu^{B\rho}G_\rho^{C\mu}$
$Q_{\widetilde{G}}$	$f^{ABC}\widetilde{G}_\mu^{A\nu}G_\nu^{B\rho}G_\rho^{C\mu}$
Q_W	$\epsilon^{IJK}W_\mu^{I\nu}W_\nu^{J\rho}W_\rho^{K\mu}$
$Q_{\widetilde{W}}$	$\epsilon^{IJK}\widetilde{W}_\mu^{I\nu}W_\nu^{J\rho}W_\rho^{K\mu}$

$2:H^6$	
Q_H	$(H^\dagger H)^3$

$3:H^4D^2$	
$Q_{H\Box}$	$(H^\dagger H)\Box(H^\dagger H)$
Q_{HD}	$\left(H^\dagger D_\mu H\right)^*\left(H^\dagger D_\mu H\right)$

$5:\psi^2H^3$ + h.c.	
Q_{eH}	$(H^\dagger H)(\bar{l}_p e_r H)$
Q_{uH}	$(H^\dagger H)(\bar{q}_p u_r \widetilde{H})$
Q_{dH}	$(H^\dagger H)(\bar{q}_p d_r H)$

$4:X^2H^2$	
Q_{HG}	$H^\dagger H\, G_{\mu\nu}^A G^{A\mu\nu}$
$Q_{H\widetilde{G}}$	$H^\dagger H\, \widetilde{G}_{\mu\nu}^A G^{A\mu\nu}$
Q_{HW}	$H^\dagger H\, W_{\mu\nu}^I W^{I\mu\nu}$
$Q_{H\widetilde{W}}$	$H^\dagger H\, \widetilde{W}_{\mu\nu}^I W^{I\mu\nu}$
Q_{HB}	$H^\dagger H\, B_{\mu\nu}B^{\mu\nu}$
$Q_{H\widetilde{B}}$	$H^\dagger H\, \widetilde{B}_{\mu\nu}B^{\mu\nu}$
Q_{HWB}	$H^\dagger\tau^I H\, W_{\mu\nu}^I B^{\mu\nu}$
$Q_{H\widetilde{W}B}$	$H^\dagger\tau^I H\, \widetilde{W}_{\mu\nu}^I B^{\mu\nu}$

$6:\psi^2XH$ + h.c.	
Q_{eW}	$(\bar{l}_p\sigma^{\mu\nu}e_r)\tau^I H W_{\mu\nu}^I$
Q_{eB}	$(\bar{l}_p\sigma^{\mu\nu}e_r)H B_{\mu\nu}$
Q_{uG}	$(\bar{q}_p\sigma^{\mu\nu}T^A u_r)\widetilde{H}\, G_{\mu\nu}^A$
Q_{uW}	$(\bar{q}_p\sigma^{\mu\nu}u_r)\tau^I\widetilde{H}\, W_{\mu\nu}^I$
Q_{uB}	$(\bar{q}_p\sigma^{\mu\nu}u_r)\widetilde{H}\, B_{\mu\nu}$
Q_{dG}	$(\bar{q}_p\sigma^{\mu\nu}T^A d_r)H G_{\mu\nu}^A$
Q_{dW}	$(\bar{q}_p\sigma^{\mu\nu}d_r)\tau^I H W_{\mu\nu}^I$
Q_{dB}	$(\bar{q}_p\sigma^{\mu\nu}d_r)H B_{\mu\nu}$

$7:\psi^2H^2D$	
$Q_{Hl}^{(1)}$	$(H^\dagger i\overleftrightarrow{D}_\mu H)(\bar{l}_p\gamma^\mu l_r)$
$Q_{Hl}^{(3)}$	$(H^\dagger i\overleftrightarrow{D}_\mu^I H)(\bar{l}_p\tau^I\gamma^\mu l_r)$
Q_{He}	$(H^\dagger i\overleftrightarrow{D}_\mu H)(\bar{e}_p\gamma^\mu e_r)$
$Q_{Hq}^{(1)}$	$(H^\dagger i\overleftrightarrow{D}_\mu H)(\bar{q}_p\gamma^\mu q_r)$
$Q_{Hq}^{(3)}$	$(H^\dagger i\overleftrightarrow{D}_\mu^I H)(\bar{q}_p\tau^I\gamma^\mu q_r)$
Q_{Hu}	$(H^\dagger i\overleftrightarrow{D}_\mu H)(\bar{u}_p\gamma^\mu u_r)$
Q_{Hd}	$(H^\dagger i\overleftrightarrow{D}_\mu H)(\bar{d}_p\gamma^\mu d_r)$
Q_{Hud} + h.c.	$i(\widetilde{H}^\dagger D_\mu H)(\bar{u}_p\gamma^\mu d_r)$

$8:(\bar{L}L)(\bar{L}L)$	
Q_{ll}	$(\bar{l}_p\gamma_\mu l_r)(\bar{l}_s\gamma^\mu l_t)$
$Q_{qq}^{(1)}$	$(\bar{q}_p\gamma_\mu q_r)(\bar{q}_s\gamma^\mu q_t)$
$Q_{qq}^{(3)}$	$(\bar{q}_p\gamma_\mu\tau^I q_r)(\bar{q}_s\gamma^\mu\tau^I q_t)$
$Q_{lq}^{(1)}$	$(\bar{l}_p\gamma_\mu l_r)(\bar{q}_s\gamma^\mu q_t)$
$Q_{lq}^{(3)}$	$(\bar{l}_p\gamma_\mu\tau^I l_r)(\bar{q}_s\gamma^\mu\tau^I q_t)$

$8:(\bar{R}R)(\bar{R}R)$	
Q_{ee}	$(\bar{e}_p\gamma_\mu e_r)(\bar{e}_s\gamma^\mu e_t)$
Q_{uu}	$(\bar{u}_p\gamma_\mu u_r)(\bar{u}_s\gamma^\mu u_t)$
Q_{dd}	$(\bar{d}_p\gamma_\mu d_r)(\bar{d}_s\gamma^\mu d_t)$
Q_{eu}	$(\bar{e}_p\gamma_\mu e_r)(\bar{u}_s\gamma^\mu u_t)$
Q_{ed}	$(\bar{e}_p\gamma_\mu e_r)(\bar{d}_s\gamma^\mu d_t)$
$Q_{ud}^{(1)}$	$(\bar{u}_p\gamma_\mu u_r)(\bar{d}_s\gamma^\mu d_t)$
$Q_{ud}^{(8)}$	$(\bar{u}_p\gamma_\mu T^A u_r)(\bar{d}_s\gamma^\mu T^A d_t)$

$8:(\bar{L}L)(\bar{R}R)$	
Q_{le}	$(\bar{l}_p\gamma_\mu l_r)(\bar{e}_s\gamma^\mu e_t)$
Q_{lu}	$(\bar{l}_p\gamma_\mu l_r)(\bar{u}_s\gamma^\mu u_t)$
Q_{ld}	$(\bar{l}_p\gamma_\mu l_r)(\bar{d}_s\gamma^\mu d_t)$
Q_{qe}	$(\bar{q}_p\gamma_\mu q_r)(\bar{e}_s\gamma^\mu e_t)$
$Q_{qu}^{(1)}$	$(\bar{q}_p\gamma_\mu q_r)(\bar{u}_s\gamma^\mu u_t)$
$Q_{qu}^{(8)}$	$(\bar{q}_p\gamma_\mu T^A q_r)(\bar{u}_s\gamma^\mu T^A u_t)$
$Q_{qd}^{(1)}$	$(\bar{q}_p\gamma_\mu q_r)(\bar{d}_s\gamma^\mu d_t)$
$Q_{qd}^{(8)}$	$(\bar{q}_p\gamma_\mu T^A q_r)(\bar{d}_s\gamma^\mu T^A d_t)$

$8:(\bar{L}R)(\bar{R}L)$ + h.c.	
Q_{ledq}	$(\bar{l}_p^j e_r)(\bar{d}_s q_{tj})$

$8:(\bar{L}R)(\bar{L}R)$ + h.c.	
$Q_{quqd}^{(1)}$	$(\bar{q}_p^j u_r)\epsilon_{jk}(\bar{q}_s^k d_t)$
$Q_{quqd}^{(8)}$	$(\bar{q}_p^j T^A u_r)\epsilon_{jk}(\bar{q}_s^k T^A d_t)$
$Q_{lequ}^{(1)}$	$(\bar{l}_p^j e_r)\epsilon_{jk}(\bar{q}_s^k u_t)$
$Q_{lequ}^{(3)}$	$(\bar{l}_p^j\sigma_{\mu\nu}e_r)\epsilon_{jk}(\bar{q}_s^k\sigma^{\mu\nu}u_t)$

Table 16. The $\mathcal{L}_6$ operators built from Standard Model fields which conserve baryon number, as given in Ref. [4]. The flavour labels of the form p,r,s,t on the Q operators are suppressed on the left hand side of the tables.